

**NASA TECHNICAL
MEMORANDUM**

NASA TM X- 71955
COPY NO.

NASA TM X- 71955

(NASA-TM-X-71955) PERFORMANCE OF LI-1542
REUSABLE SURFACE INSULATION SYSTEM IN A
HYPERSONIC STREAM (NASA) 57 p HC \$3.75

N74-23472

CSCI 20M

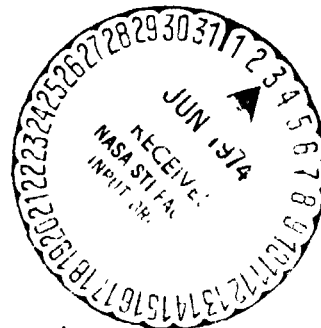
Unclas

G3/33 36950

PERFORMANCE OF LI-1542 REUSABLE SURFACE
INSULATION SYSTEM IN A HYPERSONIC STREAM

by L. Roane Hunt and Herman L. Bohon

April 1974



This informal documentation medium is used to provide accelerated or special release of technical information to selected users. The contents may not meet NASA formal editing and publication standards, may be revised, or may be incorporated in another publication.

NATIONAL AERONAUTICS AND SPACE ADMINISTRATION
LANGLEY RESEARCH CENTER, HAMPTON, VIRGINIA 23665

| | | | |
|--|--|--|---------------------------------------|
| 1. Report No. NASA TM X-71955 | 2. Government Accession No. | 3. Recipient's Catalog No. | |
| 4. Title and Subtitle PERFORMANCE OF LI-1542 REUSABLE SURFACE INSULATION SYSTEM IN A HYPERSONIC STREAM | | 5. Report Date April 1974 | 6. Performing Organization Code |
| | | 7. Author(s) L. Roane Hunt and Herman L. Bohon | 8. Performing Organization Report No. |
| 9. Performing Organization Name and Address NASA Langley Research Center Hampton, VA 23665 | | 10. Work Unit No. | 11. Contract or Grant No. |
| | | 13. Type of Report and Period Covered High-number TM-X | |
| 12. Sponsoring Agency Name and Address National Aeronautics and Space Administration Washington, D.C. 20546 | | 14. Sponsoring Agency Code | |
| | | 15. Supplementary Notes Interim technical information release subject to possible revision and/or later formal publication. | |
| 16. Abstract The thermal and structural performance of a large panel of LI-1542 reusable surface insulation tiles was determined by a series of cyclic heating tests using radiant lamps and aerothermal tests in the Langley 8-foot high-temperature structures tunnel. The test panel was designed by Lockheed Missiles and Space Company to represent a portion of the Space Shuttle Orbiter fuselage along a 1100 K isotherm. Aerothermal tests were conducted at a free-stream Mach number of 6.6, a total temperature of 1830 K, Reynolds numbers of 2.0 and 4.9×10^6 per meter, and dynamic pressures of 29 and 65 kPa. The results strongly suggest that pressure gradients in gaps and flow impingement on the header walls at the end of longitudinal gaps are sources for increased gap heating. Temperatures higher than surface radiation equilibrium temperature were measured deep in gaps and at the header walls. Also, the damage tolerance of the LI-1542 tiles appears to be very high. Cracks in the tile coating and craters from foreign particle impact had no apparent effect on tile integrity. Tile edge erosion rate was slow; however, hot gas impingement on the header walls caused excessive erosion, which could not be tolerated in a Shuttle application. Tiles soaked with water and subjected to rapid depressurization and aerodynamic heating showed no visible evidence of damage. | | | |
| 17. Key Words (Suggested by Author(s)) (STAR category underlined) <u>Thermodynamics and Combustion</u> Hypersonic Thermal Protection Surface Insulation | | 18. Distribution Statement Unclassified - unlimited | |
| 19. Security Classif. (of this report) Unclassified | 20. Security Classif. (of this page) Unclassified | 21. No. of Pages 55 | 22. Price* \$3.75 |

*Available from { The National Technical Information Service, Springfield, Virginia 22151
{ STIF/NASA Scientific and Technical Information Facility, P.O. Box 33, College Park, MD 20740

PERFORMANCE OF LI-1542 REUSABLE SURFACE
INSULATION SYSTEM IN A HYPERSONIC STREAM

by L. Roane Hunt and Herman L. Bohon
Langley Research Center

SUMMARY

The thermal and structural performance of a large panel of LI-1542 reusable surface insulation tiles was determined by a series of cyclic heating tests using radiant lamps and aerotherm^{al} tests in the Langley 8-foot high-temperature structures tunnel. The test panel was designed by Lockheed Missiles and Space Company to represent a portion of the Space Shuttle Orbiter fuselage along a 1100 K isotherm. Aerothermal tests were conducted at a free-stream Mach number of 6.6, a total temperature of 1830 K, Reynolds numbers of 2.0 and 4.9×10^6 per meter, and dynamic pressures of 29 and 65 kPa. The results strongly suggest that pressure gradients in gaps and flow impingement on the header walls at the end of longitudinal gaps are sources for increased gap heating. Temperatures higher than surface radiation equilibrium temperature were measured deep in gaps and at the header walls. Also, the damage tolerance of the LI-1542 tiles appears to be very high. Cracks in the tile coating and craters from foreign particle impact had no apparent effect on tile integrity. Tile edge erosion rate was slow; however, hot gas impingement on the header walls cause^d excessive erosion, which could not be tolerated in a Shuttle application. Tiles soaked with water and subjected to rapid depressurization and aerodynamic heating showed no visible evidence of damage.

INTRODUCTION

The thermal protection system (TPS) of the Space Shuttle has been one of the key areas of technological concern since the inception of the Shuttle program (see ref. 1) and will remain so until the system design can be verified through appropriate tests. In support of this need, a test program was initiated to assess the thermal and structural performance of candidate thermal protection systems to identify efficient design features. Several full-scale TPS models, including metallic and reusable surface insulation (RSI), were obtained from industry for thermal-structural cyclic tests in a realistic aerothermal environment. One of the RSI panels is similar to the Shuttle baseline system and test results of this system are reported herein.

The test panel consists of rigidized surface insulation tiles (designated LI-1542) bonded to a substructure. The panel was designed by Lockheed Missiles and Space Company to represent a portion of the Shuttle Orbiter fuselage along a 1100 K isotherm. The model was subjected to several thermal tests including aerodynamic and radiant heating. Aerodynamic heating tests were conducted in the Langley 8-foot high-temperature structures tunnel at a free-stream Mach number of 6.6, a total temperature of 1830 K, Reynolds numbers of 2.0 and 4.9×10^6 per meter, and dynamic pressures of 29.0 and 65.0 kPa. The radiant heating tests were performed between aerodynamic heating tests at atmospheric pressure using radiant lamps to simulate the thermal load of the entire Shuttle reentry. Preliminary test results on gap heating, flow impingement, and tile damage tolerance are reported herein.

SYMBOLS

Although physical quantities were measured in U.S. Customary Units, they are presented in this paper in the International System of Units (SI). Factors relating the two systems are given in reference 2 and in the appendix.

| | |
|------------|--|
| p | pressure, Pa |
| T | temperature, K |
| t | time, s |
| x, y, z | model coordinates (see figure 6), m |
| Δp | differential pressure load on test panel, Pa |

APPARATUS AND TESTS

Panel Description

The TPS panel consists of an array of RSI tiles bonded to stringer-stiffened beryllium subpanels mounted on a titanium frame (ref. 3). The model shown in figure 1 is 108 X 152 X 12.7 cm. The primary test article consists of 8 tiles on two subpanels. Top and bottom views of a beryllium subpanel are shown in figure 2. The subpanels are bolted on the titanium frame shown in figure 3. The frame in figure 3(a) is covered by .64 cm titanium plate around the area reserved for the two subpanels. These plates serve as a bonding surface for the peripheral tiles. An aluminum base plate (.8 mm thickness) was attached directly to the bottom of the frame to absorb the internal radiation of the test panel. The

completed metallic structure with an initial layer of silica rubber bond (RTV-560) is shown in figure 4(a). A portion of the panel with the tiles in place but not bonded is shown in figure 4(b).

The RSI tiles (designated LI-1542) are 29.11 X 29.11 X 3.18 cm and consist of rigidized silica fibers (designated LI-1500) with a .25 mm silica carbide coating (designated 0042). A schematic of the tiles and joints is shown in figure 5. The locations of the panel cross-sections are indicated in the plan view in the upper portion of the figure. The details shown are for the border joints around the subpanels, the interior panel gaps, and the common panel joint between the subpanels. (Note the offsets in the tile alignment to interrupt flow in the longitudinal gaps.) The tile edges are undercut (or notched) 1.27 cm to a height of one-half the tile thickness (or 1.59 cm) on all four sides. The surface gaps between tiles are 1.0 mm wide and the tiles are coated on the sides down to the notch. The notch is filled with a thermal seal, a soft silica fibrous material of 96 kg/m^3 density designed to prevent hot gas flow from penetrating the bond and substructure. The top of the thermal seals was coated with the 0042 coating.

Panel Instrumentation

The panel is instrumented with 65 thermocouples; 18 through the tile thickness, 27 in the tile gaps, and 20 at various locations on the substructure. The locations of these thermocouples are indicated by figure 6 and in table I. In figure 6, the plan view of the panel is shown with details of the front and rear subpanels indicated. The specific locations of thermocouples are given in table I by the cartesian coordinates and an alphanumeric system is used to identify longitudinal and lateral rows.

The longitudinal rows are jogged to follow the subpanel offset of 2.5 cm. The individual RSI tiles are identified by Roman numerals and the distribution of the thermocouples in the tiles and tile gaps are indicated by the solid symbols in the plan view. Typical in-depth thermocouples are shown in the tile, the gaps, and on the substructure in sections AA and BB at the bottom of figure 6.

Panel Holder

The panel holder is a rectangular slab with a half-wedge sharp leading edge. Flow trips at the leading edge are used to ensure an even turbulent boundary layer over the entire surface, and side plates are used to eliminate cross-flow. Flow conditions over the surface of the panel holder are described in detail in reference 4. The panel holder with the panel installed is shown in figure 7 at a typical test position, pitched at 15° to the tunnel centerline. The top surface of the test panel is set flush with the surface of the panel holder, and the panel is supported from the bottom with longitudinal structural beams. The pressure in a cavity beneath the test panel is controlled to provide differential pressure loading across the panel.

Facility

The tests were conducted in the Langley 8-foot high-temperature structures tunnel (HTST) which is shown schematically in figure 8. This facility is a hypersonic blowdown wind tunnel which uses the combustion products of methane and air as the test medium and operates at a nominal Mach number of 7, at total pressures between 3.4 and 24.1 MPa, and at nominal total temperatures between 1400 K and 2000 K. Corresponding free-stream unit Reynolds numbers are between 1×10^6 and 10×10^6 per meter.

These conditions simulate the aerothermal flight environment at Mach 7 in the altitude range between 25 and 40 km. More detailed information can be found in reference 4. A radiant heater is available in the facility to preheat the panel prior to insertion into the stream.

Tests and Test Procedures

In the normal mode of wind-tunnel operation, the model is kept out of the stream until hypersonic flow conditions are established. The model is then inserted rapidly into the stream on an elevator and programed through a sequence of events prescribed by test requirements. The model is withdrawn from the stream before tunnel shutdown.

To evaluate TPS concepts, an attempt is made to simulate a generalized temperature history associated with the Shuttle reentry trajectory. The reentry time is too long to be simulated in the relatively short test time of the 8-foot HTST; therefore, the radiant-heat apparatus is used in sequence with the wind tunnel to extend the thermal cycle. The radiant heaters are shown in the cross-section of the test chamber in figure 9. The center sketch shows the tunnel nozzle exit, test chamber, and radiant heaters. The insets show (1) the model in the wind-tunnel test position, (2) the model lowered from the test position and the radiant heaters retracted, and (3) the model covered with the radiant heaters.

Typical surface temperature histories for the three test modes are presented in figure 10. The steps which constitute a particular mode are also defined in the figure. In test mode I, thermal load is provided by radiant heaters. The temperature history of figure 10(a) is representative

of an entire Shuttle reentry thermal cycle. This cycle is characterized by a linear ramp-up of temperature in about 400 s, a temperature hold at about 1100 K for a nominal time of 1500 s, and a controlled cool-down until natural cooling becomes dominate. In test mode II, thermal loading is aerodynamically provided by the tunnel stream. The panel is inserted into the stream at ambient temperature. The surface temperature rises rapidly, approaches a steady-state level within the test duration of about 30 s, and decreases naturally after panel retraction from the stream. Mode III is a combination of mode I and mode II. The nominal hold time is 700 s and the tunnel stream exposure time is 40 s. In this test mode, close coordination is required to remove heaters and then insert the model into the test stream to minimize heat loss between heating periods.

The test panel was exposed to a total of 23 thermal cycles: 11 in mode I, 6 in mode II, and 6 in mode III. The sequence of tests and test conditions are listed in table II. For the radiant heating portions of the tests, the elapsed time during ramp-up and hold at constant surface temperature are tabulated. For the majority of aerodynamic heating tests, the total temperature was nominally 1830 K and the Reynolds number per meter was 4.9×10^6 . Nominal test conditions on the panel surface at a 15° pitch angle were a pressure of 15.2 kPa and a dynamic pressure of 171 kPa. Additional tests were also made at zero angle of attack with lower surface static and dynamic pressures. The cavity beneath the panel was, in some tests, vented to the low pressure at the base of the panel holder which developed a collapse pressure (inward acting pressure) over the panel greater than 7 kPa. In other tests, the cavity was sealed from the base

area and the collapse pressure was reduced to .7 kPa. Total test time in the aerodynamic stream is shown for each test.

RESULTS AND DISCUSSION

Thermal Response

All temperature data at a specific reference time are presented in tables III, IV, and V. Temperature data are shown at 1100 seconds into the thermal cycle for radiant heat tests only (table III, mode I) and for aerodynamic heating tests just prior to model insertion (table IV, mode III). The temperature data are grouped for ease of comparison; table III(a) and IV(a) list temperatures through the tile thickness, tables III(b) and IV(b) list temperatures in the tile gaps at 1.59 cm, and tables III(c) and IV(c) list temperatures on the support structure. Table V shows temperature data for all aerodynamic heating tests after 30 seconds in the stream for mode II and 40 seconds in the stream for mode III. It should be noted that most of the temperatures tabulated are transient; however, the surface temperatures are near steady-state.

Typical thermal response at four tile locations is shown in figure 11(a) for a mode II test (test 5) and in figure 11(b) for the aerodynamic phase of a mode III test (test 8). These locations, indicated by the inset, include the tile surface, a longitudinal border gap, and longitudinal and lateral interior gaps.

The thermal response of the border gap and the tile surface is more rapid than that of the interior gaps as indicated in figure 11(a). The maximum temperature of the border gap exceeds that of the surface. The

thermal response of the longitudinal border gap was expected to be similar to that of the longitudinal interior gap; however, this difference is attributed to hot gas leakage through the thermal seal along the border gaps (see figure 5) and will be discussed in detail in a later section.

The temperature history shown in figure 11(b) includes a portion of radiant heating for orientation. The tunnel was started while the lamps were on. During tunnel start, the local static pressure is reduced from atmospheric pressure of 100 kPa to 1.5 kPa in about 5 seconds, and the cool ambient air in the cavity beneath the panel escapes through the thermal seals along the border gaps as reflected by the sharp reduction in border gap temperature. The corresponding interior gap temperatures dropped slightly and the panel surface temperature remain unchanged during this reduction in static pressure. After model insertion, the surface temperature quickly reaches steady-state, or radiation equilibrium, and the border gap temperature (as noted in figure 11(a)) again exceeds the tile surface temperature.

The gap temperatures (solid symbols) and tile temperatures at a depth of 1.27 cm (square symbols) for test 8 are displayed on plan views of the tile array in figure 12. These temperatures are listed in tables IV and V. For comparison, the temperatures recorded at $t = 1100$ seconds into the radiant heating phase are presented in figure 12(a) and corresponding temperatures recorded at $t = 1215$ seconds (see time scale of figure 11(b)) are presented in figure 12(b). Generally, the temperatures shown in figure 12(a) are relatively uniform at about 800 K as compared to a surface temperature of approximately 1100 K (table IV). As indicated in figure 12(b), the temperature changed radically during the aerodynamic heating phase.

Temperatures near 1400 K were recorded along the longitudinal border gaps (rows 1 and 5); however, temperatures of the interior gaps (both longitudinal and lateral) were generally around 900 K to 1000 K. The high temperatures at the "header" region - that is, the forward-facing wall at the end of longitudinal gap (for instance, the intersections of rows A3, E3, and I3) - were about 1350 K. The gap temperatures of the header region were expected to be higher than the other gap temperatures because the header region served as a stagnation surface for longitudinal gap flow. The lateral gap temperatures adjacent to the headers in rows A, E, and I are 100 K to 200 K less than the header temperatures, but are generally greater than the interior gap temperatures.

Effects of Differential Pressure

The longitudinal border and subpanel gap temperatures were considerably higher than expected and suggest increased gap flow due to leakage through the thermal seals which permitted hot gas flowthrough to the substructure. The border gap temperature distribution along row 5 is shown in figure 13 for two differential pressure loadings, $\Delta p = 7.6$ kPa (test 8) and Δp (test 22). The difference in the temperature levels is indicative of increased gap flow as a result of seal leakage. Reducing the differential pressure resulted in a 100 K to 300 K reduction in border gap temperatures. The substructure temperature at E5 was 500 K during run 8 ($\Delta p = 7.6$ kPa) but only 300 K during test 22 ($\Delta p = .7$ kPa). Consequently, hot gas was apparently leaking to the substructure at E5 where lateral and longitudinal border seals meet. The effects of flow leakage along the longitudinal border gaps on lateral gap temperatures are shown in figure 14 where temperatures along row E are plotted for tests 8 and 22. The header temperature at $y = 0$ is

unaffected by Δp . However, the adjacent temperatures, about 15 cm on each side, show 200 K to 300 K reductions when Δp is reduced. Note the difference in the substructure temperatures indicates flowthrough at both corners E1 and E5. These data strongly suggest that gas leakage at the corners causes gap flow transverse to the stream direction. The influence of transverse flow on gap temperature is dependent on the energy of flow in the longitudinal gap approaching the header, which is characterized by the temperature and pressure at the header region.

The interior panel lateral gap temperatures in row G are shown in figure 15 for tests 8 and 22. Here, the effect of pressure gradient is seen to be small due primarily to the absence of an offset (or header) in the longitudinal gap at the center of the subpanel.

After completion of all the tests, the panel was disassembled to examine the regions where hot gas flowed through the thermal seals. The tile array with the forward subpanel removed is shown in figure 16. Much of the fibrous thermal seal was damaged during disassembly. The deep seal in the lateral gap (row E) does not extend to the corner (E5) where high substructure temperatures were noted in figure 14. Evidence of hot gas flow in this region includes an appearance of scrubbing action on the thermal seal and discoloration of the substructure caused by out-gassing of the RTV bond material.

Tile Damage Tolerance

During the test series, the tiles incurred considerable surface damage. In spite of all the surface damage, the array still provided good thermal

performance and appears to have adequate structural integrity. The overall appearance of the tile surface at the conclusion of the tests is shown by the photograph in figure 17. Because of the severity of the test conditions, subsequent tests following the event of surface damage provides some insight into the damage tolerance of the LI-1542 material.

Tile protective coating damage. - The coating is intended to protect the tile from water ingress and to prevent shear erosion of the basic silica tile. Although invisible to the naked eye, cracks were found in the coating before test 4, as indicated in figure 18(a) where the crack pattern is traced on a transparency. During test 4, tunnel flame-out occurred after 6.2 seconds in the stream (see table II); consequently, the hot tiles were exposed to extremely cold flow. A photograph of a typical tile crack pattern after test 4 is shown in figure 18(b). The tile is wetted by a volatile solvent to expose the hairline cracks. All of the tiles were crazed as shown in figure 18(b) after run 4, but did not seem to worsen with repeated tests. There was no flaking of the RSI which suggests the cracks did not penetrate the basic silica tile.

Effects of water soak. - Since the coating crazed and consequently could allow water ingress, tiles VI and VIII were soaked with water for test 23 to determine its effect on tile integrity during rapid change in pressure and temperature. The static pressure and temperature histories for tile VIII are shown in figure 19. The depressurization from 100 kPa to 1.5 kPa occurs during tunnel startup and is followed by a pressure increase as the model is inserted into the stream. For comparison, the Shuttle ascent depressurization rate is shown by the dashed curve. The surface temperature histories

of the soaked tile and an adjacent tile (tile V) with no water are shown on the right of the figure. The temperature of the soaked tile leveled off at the boiling point of water at the local static pressure. However, it is possible that the thermocouple in the soaked tile was shorted by the water; consequently, the surface temperature may have been greater than that shown. Nevertheless, an excessive amount of water was absorbed in the tile and the depressurization rate experienced by the tile was extreme without any evidence of damage to the tile surface.

Foreign particle impact. - During the wind tunnel tests, the model was bombarded with foreign particles inadvertently produced by flaking of the thermal coating of the combustor liner of the 8-foot HTST. Impact of these minute particles caused extensive crater damage to the tiles. A series of photos is shown in figure 20 to illustrate the progression of surface damage. The photos were taken of the same tile after test 8, 12, and 23. The large crater (see large arrow), which appeared after test 8, was field repaired with a mixture of the coating material, and no further erosion was experienced. A smaller crater (see small arrow), which also appeared after run 8, was not repaired and showed no evidence of erosion for the remainder of the tests. Thus, particle impact which caused craters in the RSI tiles had no discernible effect on the tile integrity.

Edge erosion. - The tile assembly had forward-facing steps at two locations; each of which experienced erosion along the tile edges. The progression of edge erosion of a .6 mm step and a .4 mm step is shown in figures 21 and 22, respectively. The propagation of the edge erosion was probably enhanced by foreign particle impact, however, the erosion rate was slow and exposure

of the bare silica to the stream did not result in catastrophic failure. Observation of movie film indicated the eroded edges became local hot spots because of the reduced value of emissivity in the absence of coating.

Flow impingement. - At least one type of damage which cannot be tolerated during a reentry is that due to hot gas impingement in the header region. As noted earlier, temperature at the bottom of the gaps in the header region measured about 1350 K. The resulting damage is shown in figure 23 where the forward-facing wall at the intersection of rows E3 has been eroded about 1 cm into the silica. The temperature in this region must have been near the melting temperature of the silica. This erosion and similar ones at other header regions are significant in the fact that the surface temperature of the tiles was only 1100 K. Consequently, along the bottom centerline of the Orbiter where surface temperatures are around 1600 K, impingement of gap flow on a forward-facing wall could be catastrophic.

CONCLUDING REMARKS

A large panel of LI-1542 RSI tiles was subjected to a series of cyclic heating tests using radiant lamps and aerotherm tests in the 8-foot high-temperature structures tunnel to assess their thermal and structural performance. The results strongly suggest that pressure gradients in gaps and flow impingement on the header walls at the end of longitudinal gaps are sources for increased gap heating. Temperatures higher than the surface radiation equilibrium temperature were measured deep in gaps and at header walls. Also, the damage tolerance of LI-1542 RSI appears to be very high. The silica carbide coating became crazed early in the test program, but had

no apparent effect on tile integrity. Impact of foreign particles in the stream caused craters in the tiles, but field repairs successfully retarded erosion of the impacted area. Tile edge erosion rate was slow and exposure of the bare silica to the stream did not result in catastrophic failure. However, hot gas impingement on the header walls caused excessive erosion, which could not be tolerated in a Shuttle application. Tiles soaked with water and subjected to rapid depressurization and aerodynamic heating showed no visible evidence of damage.

APPENDIX

CONVERSION OF U.S. CUSTOMARY UNITS TO SI UNITS

Factors required for converting U.S. Customary Units to the International System of Units (SI) are given in the following table:

| Physical quantity | U.S. Customary Unit | Conversion factor (*) | SI Unit |
|-------------------|-----------------------|-----------------------|--|
| Density | pcf | 16.01846 | kilogram/meter ³ (kg/m ³) |
| Length | { in. ft per ft | 0.0254 | meter (m) |
| | | 0.3048 | meter (m) |
| | | 3.28083 | per meter (m ⁻¹) |
| Pressure | psi | 6894.757 | pascal (Pa) |
| Temperature | °R | 5/9 | kelvin (K) |

*Multiply value in U.S. Customary Unit by conversion factor to obtain equivalent value in SI Unit.

Prefixes to indicate multiples of units are as follows:

| Prefix | Multiple |
|-----------|------------------|
| kilo (k) | 10 ³ |
| centi (c) | 10 ⁻² |
| milli (m) | 10 ⁻³ |

REFERENCES

1. Anderson, Roger A.; Brooks, William A.; Leonard, Robert W.; and Maltz, Joseph: Structures - A Technology Overview. *Astronautics and Aeronautics*, Vol. 9, No. 2, February 1971, pp. 38-47.
2. Anon.: Metric Practice Guide. E 380-72, Amer. Soc. Testing Mater., June 1972.
3. Eurns, A. Bruce: Final Report for Structural Evaluation of Candidate Space Shuttle Thermal Protection Systems. Rep. No. LMSC-D157398 (Contract NAS1-11153) Lockheed Missiles and Space Company, June 26, 1972.
4. Deveikis, William D.; and Hunt, L. Roane: Loading and Heating of Large Flat Plate at Mach 7 in the Langley 8-foot High-Temperature Structures Tunnel. NASA TN D-7275, 1973.

TABLE I.- THERMOCOUPLE LOCATIONS
(a) RSI tile

| Thermocouple No. | Tile no. | Row | x, cm | y, cm |
|-------------------|----------|-----|-------|-------|
| $z = 0$ (surface) | | | | |
| T8 | I | B2 | 32.4 | -10.8 |
| T10 | III | B4 | 32.4 | 13.3 |
| T21 | IV | D4 | 61.8 | 15.9 |
| T28 | V | F2 | 90.8 | -15.9 |
| T30 | VII | F4 | 90.8 | 13.3 |
| T39 | VI | H2 | 120.0 | -13.3 |
| T41 | VIII | H4 | 120.0 | 10.8 |
| $z = .51$ cm | | | | |
| T5 | I | B2 | 32.4 | -13.3 |
| T11 | III | B4 | 32.4 | 15.9 |
| T36 | VI | H2 | 120.0 | -15.9 |
| T42 | VIII | H4 | 120.0 | 13.3 |
| $z = 1.27$ cm | | | | |
| T6 | I | B2 | 32.4 | -13.3 |
| T12 | III | B4 | 32.4 | 15.9 |
| T43 | VIII | H4 | 120.0 | 13.3 |
| $z = 2.29$ cm | | | | |
| T7 | I | B2 | 32.4 | -13.3 |
| T13 | III | B4 | 32.4 | 15.9 |
| T38 | VI | H2 | 120.0 | -15.9 |
| T44 | VIII | H4 | 120.0 | 13.3 |

TABLE I.- THERMOCOUPLE LOCATION - Continued
 (b) RSI tile gap ($z = 1.59\text{cm}$)

| Thermocouple No. | Tile no. | Row | x, cm | y, cm |
|---------------------|----------|-----|-------|-------|
| Border gap, row A | | | | |
| T1 | I | A2 | 17.8 | -13.3 |
| T2 | I | A3 | ↓ | 1.3 |
| T3 | III | A4 | | 15.9 |
| Subpanel gap, row E | | | | |
| T23 | V | E2 | 76.2 | -15.9 |
| T24 | V | E3 | ↓ | - 1.3 |
| T25 | VII | E3 | | 1.3 |
| T26 | VII | E4 | | 15.9 |
| Border gap, row I | | | | |
| T46 | VI | I 2 | 134.6 | -15.9 |
| T47 | VI | I 3 | ↓ | - 1.3 |
| T48 | VIII | I 4 | | 13.3 |
| Border gap, row 1 | | | | |
| T4 | I | B1 | 32.4 | -27.9 |
| T18 | II | D1 | 61.8 | -27.9 |
| T27 | V | F1 | 90.8 | -30.5 |
| T35 | VI | H1 | 120.0 | -30.5 |
| Border gap, row 5 | | | | |
| T14 | III | B5 | 32.4 | 30.5 |
| T22 | IV | D5 | 61.8 | 30.5 |
| T31 | VII | F5 | 90.8 | 27.9 |
| T45 | VIII | H5 | 120.0 | 27.9 |
| Interior gaps | | | | |
| T9 | III | B3 | 32.4 | 1.3 |
| T15 | II | C7 | 47.0 | -13.3 |
| T16 | II | C3 | ↓ | 1.3 |
| T17 | IV | C4 | | 15.9 |
| T20 | IV | D3 | 61.8 | 1.3 |
| T32 | V | D2 | 105.4 | -15.9 |
| T33 | V | D3 | ↓ | - 1.3 |
| T34 | VII | D4 | | 13.3 |
| T40 | VIII | H3 | 120.0 | - 1.3 |

| TABLE I. - THERMOCOUPLE LOCATIONS - Concluded (c) Substructure | | |
|---|-------|-------|
| Thermocouple No. | x, cm | y, cm |
| Beryllium subpanel skin (z = 3.50 cm) | | |
| T81 | 32.4 | 2.5 |
| T82 | 32.4 | 0 |
| T85 | 105.4 | 6.7 |
| Titanium frame (z = 6.78 cm) | | |
| T59 | 20.3 | 0 |
| T61 | 78.7 | -27.9 |
| T63 | ↓ | 0 |
| T65 | ↓ | 25.4 |
| T67 | 105.4 | -27.9 |
| T69 | 105.4 | 25.4 |
| T71 | 132.1 | -27.9 |
| Titanium frame (z = 12.6 cm) | | |
| T60 | 20.3 | 0 |
| T62 | 78.7 | -27.9 |
| T64 | ↓ | 0 |
| T66 | ↓ | 25.4 |
| T68 | 105.4 | -27.9 |
| T70 | 105.4 | 25.4 |
| T72 | 132.1 | -27.9 |
| T74 | 132.1 | 0 |
| Aluminum base plate (z = 12.7 cm) | | |
| T77 | 47.0 | 0 |
| T78 | 105.4 | 0 |

TABLE II. - SEQUENCE OF TESTS AND TEST CONDITIONS OF THE LI-1542 PANEL

| Test | Mode* | Radiant Heat | | Wind Tunnel | | Model | | | | | Comments |
|------|-------|-----------------|--------------|----------------------|------------------------|--------------------------|-----------------------|-----------------------------|------------------------|-------------------|--------------------|
| | | Ramp-up time, s | Hold time, s | Total temperature, K | Reynolds No. per meter | Angle of Attack, Degrees | Surface Pressure, kPa | Local Dynamic Pressure, kPa | Collapse Pressure, kPa | Time in stream, s | |
| 1 | I | 340 | 350 | 1830 | 2.0x10 ⁶ | 0 | .90 | 29.4 | 0 | 2.85 | Tunnel Breakdown |
| 2 | II | | | 1800 | 2.0 | 0 | .90 | 29.4 | .2 | 45.8 | |
| 3 | II | | | 1770 | 4.9 | 15 | 15.2 | 171. | 8.6 | 6.2 | Combustor flameout |
| 4 | II | | | 1830 | 4.9 | 15 | 15.2 | 171. | 8.8 | 29.8 | |
| 5 | II | | | 1800 | 4.9 | 15 | 15.2 | 171. | 8.6 | 42.6 | |
| 6 | II | | | | | | | | | | |
| 7 | I | 380 | 780 | 1830 | 4.9 | 15 | 15.2 | 171. | 7.6 | 39.8 | |
| 8 | III | 380 | 790 | | | | | | | | |
| 9 | I | 380 | 1270 | | | | | | | | |
| 10 | III | 430 | 670 | 1830 | 4.9 | 15 | 15.2 | 171. | 7.2 | 38.2 | |
| 11 | III | 460 | 950 | 1800 | 4.9 | 0 | 2.1 | 65.3 | -9 | 40.6 | |
| 12 | III | 440 | 650 | 1800 | 4.9 | 15 | 15.2 | 171. | 5.2 | 39.7 | |
| 13 | I | 530 | 1410 | | | | | | | | |
| 14 | I | 450 | 630 | | | | | | | | |
| 15 | III | 420 | 650 | 1830 | 4.9 | 15 | 15.2 | 171. | 8.8 | 40.0 | |
| 16 | I | 450 | 1280 | | | | | | | | |
| 17 | I | 430 | 650 | | | | | | | | |
| 18 | I | 440 | 620 | | | | | | | | |
| 19 | I | 430 | 760 | | | | | | | | |
| 20 | I | 450 | 160 | | | | | | | | |
| 21 | I | 410 | 1800 | 1830 | 4.9 | 15 | 15.2 | 171. | .7 | 40.6 | Water in two tiles |
| 22 | III | 430 | 1070 | 1800 | 4.9 | 15 | 15.2 | 171. | .7 | 30.6 | |
| 23 | II | | | | | | | | | | |

- I - Radiant heating
- II - Aerodynamic heating
- III - Radiant and aerodynamic heating

TABLE III - MODE I PANEL TEMPERATURES (K) AT $t \approx 1100$ s.
(a) RSI tile

| Thermo- couple No. | Test No. | | | | | | | | |
|--------------------------|----------|------|------|------|------|------|------|------|------|
| | 7 | 9 | 13 | 14 | 16 | 17 | 18 | 19 | 20 |
| $z = 0$ (surface) | | | | | | | | | |
| T8 | 1102 | 1117 | 1109 | 1103 | 1126 | 1111 | 1108 | 1112 | 1084 |
| T10 | — | — | 1054 | 1049 | 1069 | 1057 | 1053 | 1058 | — |
| T21 | 1052 | 1065 | 1052 | 1049 | 1066 | 1055 | 1055 | 1060 | 1027 |
| T28 | 1045 | 1055 | 1039 | 1039 | 1061 | 1057 | 1051 | 1063 | 1031 |
| T30 | — | — | — | — | — | — | — | — | — |
| T39 | 1116 | 1126 | 1116 | 1101 | 1132 | 1119 | 1109 | 1123 | 1101 |
| T41 | 1114 | 1123 | 1121 | 1108 | 1136 | 1117 | 1113 | 1116 | 1099 |
| $z = .51$ cm | | | | | | | | | |
| T5 | 1027 | 1042 | 1026 | 1026 | 1047 | 1031 | 1033 | 1031 | 1006 |
| T11 | 965 | 978 | 959 | 962 | 978 | 966 | 968 | 966 | 942 |
| T36 | 1028 | 1039 | 1023 | 1018 | 1043 | 1031 | 1025 | 1032 | 1010 |
| T42 | 1033 | 1035 | 1029 | 1020 | 1047 | 1027 | 1028 | 1024 | 1011 |
| $z = 1.27$ cm | | | | | | | | | |
| T6 | 848 | 859 | 831 | 841 | 858 | 844 | 845 | 823 | 822 |
| T12 | 797 | 808 | 776 | 789 | 804 | 792 | 793 | 790 | 769 |
| T43 | 869 | 876 | 854 | 858 | 878 | 862 | 862 | 859 | 844 |
| $z = 2.29$ cm | | | | | | | | | |
| T7 | 263 | 608 | 574 | 588 | 599 | 593 | 589 | 586 | 570 |
| T13 | 564 | 571 | 537 | 551 | 561 | 554 | 550 | 547 | 533 |
| T38 | 613 | 559 | 587 | 600 | 611 | 607 | 598 | 601 | 586 |
| T44 | 621 | 628 | 598 | 609 | 622 | 613 | 608 | 606 | 593 |

TABLE III.- MODE I PANEL TEMPERATURES (K) AT $t \approx 1100$ s -Continued
 (b) RSI tile gap ($z = 1.59$ cm)

| Thermo- couple No. | Test No. | | | | | | | | |
|--------------------------|----------|-----|-----|-----|-----|-----|-----|-----|-----|
| | 7 | 9 | 13 | 14 | 16 | 17 | 18 | 19 | 20 |
| Border gap, row A | | | | | | | | | |
| T1 | 777 | 808 | 792 | 766 | 807 | 753 | 765 | 757 | 694 |
| T2 | 658 | 736 | 707 | 549 | 674 | 469 | 526 | 492 | 408 |
| T3 | 785 | 818 | 794 | 729 | 794 | 697 | 726 | 729 | 636 |
| Subpanel gap, row E | | | | | | | | | |
| T23 | 832 | 844 | 816 | 814 | 838 | 818 | 826 | 826 | 797 |
| T24 | 826 | 860 | 832 | 813 | 850 | 802 | 824 | 816 | 743 |
| T25 | 867 | 891 | 856 | 852 | 877 | 847 | 863 | 859 | 812 |
| T26 | 867 | 894 | 869 | 854 | 894 | 857 | 868 | 864 | 801 |
| Border gap, row I | | | | | | | | | |
| T46 | 819 | 833 | 803 | 798 | 827 | 805 | 799 | 803 | 768 |
| T47 | 787 | 811 | 779 | 732 | 789 | 693 | 731 | 731 | 608 |
| T48 | 833 | 847 | 826 | 823 | 844 | 820 | 822 | 819 | 788 |
| Border gap, row 1 | | | | | | | | | |
| T4 | 758 | 798 | 768 | 699 | 786 | 669 | 701 | 682 | 536 |
| T18 | 754 | 791 | 753 | 738 | 772 | 713 | 754 | 744 | 688 |
| T27 | 692 | 734 | 696 | 589 | 709 | 584 | 618 | 632 | 509 |
| T35 | 713 | 737 | 715 | 642 | 733 | 674 | 648 | 689 | 620 |
| Border gap, row 5 | | | | | | | | | |
| T14 | 740 | 774 | 748 | 695 | 763 | 686 | 692 | 705 | 604 |
| T22 | 795 | 816 | 788 | 788 | 815 | 787 | 767 | 791 | 743 |
| T31 | 694 | 744 | 721 | 659 | 739 | 680 | 669 | 693 | 602 |
| T45 | 742 | 787 | 764 | 703 | 781 | 719 | 703 | 726 | 616 |
| Interior gaps | | | | | | | | | |
| T9 | 806 | 815 | 787 | 796 | 809 | 794 | 795 | 791 | 760 |
| T15 | 873 | 892 | 861 | 865 | 888 | 865 | 869 | 864 | 829 |
| T16 | 959 | 975 | 947 | 953 | 974 | 957 | 952 | 949 | 916 |
| T17 | 816 | 832 | 806 | 807 | 831 | 809 | 811 | 809 | 774 |
| T20 | 804 | 818 | 787 | 802 | 814 | 805 | 805 | 803 | 777 |
| T32 | 867 | 880 | 846 | 853 | 875 | 862 | 858 | 861 | 837 |
| T33 | 867 | 877 | 856 | 861 | 881 | 866 | 866 | 868 | 843 |
| T34 | 889 | 901 | 876 | 880 | 904 | 887 | 886 | 884 | 865 |
| T40 | 796 | 807 | 777 | 782 | 803 | 789 | 789 | 791 | 768 |

TABLE III.- MODE I PANEL TEMPERATURES (K) AT $t \approx 1100$ s - Concluded
(c) Substructures

| Thermo- couple No. | Test No. | | | | | | | | |
|--|----------|-----|-----|-----|-----|-----|-----|-----|-----|
| | 7 | 9 | 13 | 14 | 16 | 17 | 18 | 19 | 20 |
| Beryllium subpanel skin ($z = 3.50$ cm) | | | | | | | | | |
| T81 | 359 | 364 | 341 | 352 | 354 | 356 | 345 | 342 | 336 |
| T82 | 360 | 366 | 342 | 353 | 356 | 358 | 347 | 343 | 336 |
| T85 | 372 | 377 | 352 | 362 | 367 | 369 | 357 | 356 | 349 |
| Titanium frame ($z = 6.78$ cm) | | | | | | | | | |
| T59 | 317 | 324 | 308 | 317 | 317 | 322 | 309 | 307 | 302 |
| T61 | 311 | 318 | 302 | 311 | 311 | 317 | 304 | 302 | 297 |
| T63 | 321 | 328 | 311 | 319 | 320 | 325 | 313 | 311 | 306 |
| T65 | 316 | 323 | 306 | 316 | 316 | 321 | 308 | 306 | 301 |
| T67 | 310 | 317 | 301 | 311 | 310 | 316 | 303 | 302 | 297 |
| T69 | 312 | 319 | 303 | 313 | 312 | 318 | 306 | 304 | 299 |
| T71 | 312 | 318 | 313 | 312 | 312 | 317 | 305 | 303 | 295 |
| Titanium frame ($z = 12.6$ cm) | | | | | | | | | |
| T60 | 296 | 305 | 292 | 303 | 299 | 309 | 294 | 293 | 289 |
| T62 | 296 | 305 | 291 | 301 | 299 | 309 | 293 | 292 | 289 |
| T64 | 296 | 304 | 292 | 302 | 299 | 309 | 294 | 293 | 289 |
| T66 | 296 | 303 | 291 | 302 | 298 | 308 | 293 | 292 | 288 |
| T68 | 296 | 305 | 291 | 301 | 298 | 308 | 294 | 292 | 288 |
| T70 | 296 | 304 | 291 | 301 | 298 | 308 | 294 | 292 | 288 |
| T72 | 296 | 304 | 291 | 300 | 298 | 307 | 293 | 292 | 288 |
| T74 | 295 | 303 | 291 | 300 | 298 | 307 | 293 | 292 | 288 |
| Aluminum base plate ($z = 12.7$ cm) | | | | | | | | | |
| T77 | 298 | 307 | 293 | 304 | 301 | 311 | 296 | 294 | 291 |
| T78 | 298 | 306 | 292 | 302 | 300 | 309 | 295 | 294 | 290 |

TABLE IV. - MODE III PANEL TEMPERATURES (K) AT + \approx 1100 s
(a) RSI tile

| Thermo- couple No. | Test No. | | | | | |
|--------------------------|----------|------|------|------|------|------|
| | 8 | 10 | 11 | 12 | 15 | 22 |
| $z = 0$ (surface) | | | | | | |
| T8 | 1111 | 1115 | 1114 | 1076 | 1107 | 1101 |
| T10 | - | 1064 | 1065 | 1026 | 1052 | - |
| T21 | 1101 | 1070 | 1058 | 1023 | 1052 | 1042 |
| T28 | 1092 | 1057 | 1057 | 1018 | 1050 | 1032 |
| T30 | 1109 | - | - | - | - | - |
| T39 | 1125 | 1116 | 1119 | 1080 | 1115 | 1094 |
| T41 | 1124 | 1116 | 1120 | 1182 | 1117 | 1096 |
| $z = .51$ cm | | | | | | |
| T5 | 1035 | 1040 | 1037 | 997 | 1029 | 1031 |
| T11 | 981 | 978 | 975 | 936 | 964 | 961 |
| T36 | 1037 | 1032 | 1032 | 991 | 1029 | 1015 |
| T42 | 1037 | 1031 | 1032 | 994 | 1027 | 1018 |
| $z = 1.27$ cm | | | | | | |
| T6 | 852 | 856 | 850 | 815 | 836 | 844 |
| T12 | 808 | 806 | 801 | 766 | 785 | 788 |
| T43 | 876 | 870 | 868 | 833 | 858 | 855 |
| $z = 2.29$ cm | | | | | | |
| T7 | 601 | 602 | 595 | 572 | 584 | 593 |
| T13 | 567 | 564 | 558 | 537 | 546 | 554 |
| T38 | 615 | 612 | 608 | 584 | 598 | 600 |
| T44 | 624 | 621 | 616 | 592 | 606 | 609 |

TABLE IV. - MODE III PANEL TEMPERATURES (K) AT $t \approx 1100$ s - Continued
 (b) RSI tile gap ($z = 1.59$ cm)

| Thermo- couple No. | Test No. | | | | | |
|--------------------------|----------|-----|------|-----|-----|-----|
| | 8 | 10 | 11 | 12 | 15 | 22 |
| Border gap, row A | | | | | | |
| T1 | 819 | 783 | 780 | 744 | 754 | 673 |
| T2 | 820 | 618 | 561 | 543 | 507 | 409 |
| T3 | 841 | 782 | 765 | 724 | 718 | 611 |
| Subpanel gap, row E | | | | | | |
| T23 | 873 | 842 | 827 | 797 | 821 | 799 |
| T24 | 899 | 829 | 820 | 782 | 800 | 748 |
| T25 | 916 | 868 | 860 | 824 | 849 | 824 |
| T26 | 926 | 878 | 871 | 828 | 847 | 810 |
| Border gap, row I | | | | | | |
| T46 | 830 | 821 | 815 | 772 | 802 | 771 |
| T47 | 831 | 774 | 750 | 713 | 733 | 590 |
| T48 | 846 | 836 | 833 | 798 | 818 | 794 |
| Border gap, row 1 | | | | | | |
| T4 | 819 | 752 | 740 | 682 | 669 | 331 |
| T18 | 813 | 771 | 756 | 721 | 736 | 692 |
| T27 | 769 | 681 | 680 | 627 | 612 | 502 |
| T35 | 762 | 703 | 706 | 666 | 681 | 586 |
| Border gap, row 5 | | | | | | |
| T14 | 799 | 745 | 733 | 695 | 699 | 596 |
| T22 | 847 | 806 | 799 | 739 | 784 | 756 |
| T31 | 779 | 713 | 708 | 761 | 684 | 608 |
| T45 | 812 | 757 | 750 | 627 | 721 | 620 |
| Interior gaps | | | | | | |
| T9 | 818 | 812 | 804 | 744 | 794 | 775 |
| T15 | 896 | 884 | 877 | 803 | 863 | 851 |
| T16 | 983 | 973 | 967 | 879 | 957 | 932 |
| T17 | 849 | 827 | 819 | 728 | 804 | 793 |
| T20 | 834 | 813 | 813 | 764 | 802 | 796 |
| T32 | 885 | 872 | 867 | 809 | 853 | 848 |
| T33 | 896 | 877 | 874 | 811 | 865 | 857 |
| T34 | 908 | 896 | 892 | 842 | 884 | 877 |
| T40 | 811 | 801 | 1120 | 753 | 788 | 779 |

TABLE IV.- MODE III PANEL TEMPERATURES (K) AT $t \approx 1100$ s - Concluded
(c) Substructure

| Thermo- couple No. | Test No. | | | | | |
|--|----------|-----|-----|-----|-----|-----|
| | 8 | 10 | 11 | 12 | 15 | 22 |
| Beryllium subpanel skin ($z = 3.50$ cm) | | | | | | |
| T81 | 361 | 358 | 353 | 344 | 344 | 357 |
| T82 | 362 | 360 | 327 | 346 | 346 | 358 |
| T85 | 374 | 371 | 366 | 357 | 357 | 402 |
| Titanium frame ($z = 6.78$ cm) | | | | | | |
| T59 | 323 | 320 | 316 | 310 | 309 | 321 |
| T61 | 317 | 314 | 306 | 304 | 304 | 316 |
| T63 | 327 | 323 | 319 | 314 | 313 | 323 |
| T65 | 323 | 318 | 316 | 308 | 308 | 320 |
| T67 | 317 | 314 | 310 | 303 | 304 | 315 |
| T69 | 318 | 316 | 312 | 306 | 306 | 317 |
| T71 | 317 | 315 | 312 | 306 | 306 | 316 |
| Titanium frame ($z = 12.6$ cm) | | | | | | |
| T60 | 305 | 303 | 299 | 294 | 294 | 306 |
| T62 | 301 | 303 | 299 | 293 | 294 | 306 |
| T64 | 305 | 303 | 299 | 294 | 294 | 306 |
| T66 | 304 | 303 | 299 | 293 | 294 | 307 |
| T68 | 304 | 303 | 299 | 293 | 294 | 305 |
| T70 | 304 | 302 | 299 | 293 | 294 | 306 |
| T72 | 303 | 302 | 298 | 293 | 293 | 303 |
| T74 | 303 | 301 | 298 | 293 | 294 | 302 |
| Aluminum frame ($z = 12.7$ cm) | | | | | | |
| T77 | 307 | 305 | 301 | 296 | 296 | 309 |
| T78 | 306 | 303 | 300 | 295 | 296 | 306 |

TABLE V. - PANEL TEMPERATURES (K) AFTER 30 s OF AERODYNAMIC HEATING
 FOR MODE II AND 40 s OF AERODYNAMIC HEATING FOR MODE III
 (a) RSI tile

| Thermo- couple no. | Test no. | | | | | | | | | |
|--------------------------|----------|------|------|------|------|-----|------|------|------|------|
| | 3 | 5 | 6 | 8 | 10 | 11 | 12 | 15 | 22 | 23 |
| $z = 0$ (surface) | | | | | | | | | | |
| T8 | 732 | 1139 | 1126 | 1187 | 1166 | 953 | 1160 | 1173 | 1210 | 1150 |
| T10 | 684 | - | - | - | 1157 | 949 | 1149 | 1162 | - | 1101 |
| T21 | 766 | 1239 | 699 | 1201 | 1204 | 943 | 1160 | 1178 | 1205 | 1149 |
| T28 | 694 | 1093 | 1081 | 1176 | 1152 | 938 | 1146 | 1161 | 1180 | 1100 |
| T30 | - | 1127 | 1109 | 1182 | - | - | - | - | - | - |
| T39 | 699 | 1113 | 1102 | 1186 | 1163 | 940 | 1156 | 1173 | 1191 | 396 |
| T41 | 667 | 1089 | 1074 | 1183 | 1162 | 780 | 1158 | 1176 | 1189 | 351 |
| $z = .51$ cm | | | | | | | | | | |
| T5 | 370 | 613 | 609 | 1061 | 1049 | 950 | 1037 | 1052 | 1080 | 637 |
| T11 | 329 | 479 | 478 | 1007 | 984 | 922 | 971 | 989 | 1014 | 503 |
| T36 | 359 | 598 | 594 | 1056 | 1039 | 937 | 1028 | 1048 | 1057 | 337 |
| T42 | 352 | 582 | 852 | 1046 | 1028 | 938 | 1020 | 1039 | 1052 | 334 |
| $z = 1.27$ cm | | | | | | | | | | |
| T6 | 293 | 294 | 292 | 858 | 908 | 848 | 819 | 1093 | 873 | 295 |
| T12 | 294 | 292 | 290 | 821 | 804 | 809 | 769 | 790 | 819 | 292 |
| T43 | 294 | 303 | 319 | 877 | 862 | 856 | 838 | 862 | 879 | 334 |
| $z = 2.29$ cm | | | | | | | | | | |
| T7 | 293 | 292 | 291 | 620 | 607 | 626 | 577 | 591 | 638 | 290 |
| T13 | 293 | 291 | 290 | 588 | 567 | 591 | 541 | 552 | 598 | 290 |
| T38 | 293 | 291 | 289 | 633 | 616 | 632 | 588 | 606 | 639 | 337 |
| T44 | 293 | 291 | 289 | 639 | 623 | 638 | 597 | 613 | 648 | 333 |

TABLE V. - PANEL TEMPERATURES (K) AFTER 30 s OF AERODYNAMIC HEATING FOR MODE II AND 40 s OF AERODYNAMIC HEATING FOR MODE III - Continued
(b) RSI tile gap (z = 1.59 cm)

| Thermo- couple no. | Test no. | | | | | | | | | |
|--------------------------|----------|------|------|------|------|-----|------|------|------|------|
| | 3 | 5 | 6 | 8 | 10 | 11 | 12 | 15 | 22 | 23 |
| Border gap, row A | | | | | | | | | | |
| T1 | 291 | 507 | 523 | 859 | 804 | 697 | 676 | 835 | 500 | 299 |
| T2 | 293 | 1138 | 1112 | 1274 | 1247 | 509 | 1191 | 1278 | 767 | 497 |
| T3 | 291 | 588 | 594 | 1042 | 998 | 634 | 954 | 996 | 591 | 406 |
| Subpanel gap, row E | | | | | | | | | | |
| T23 | 293 | 923 | 920 | 1146 | 1095 | 771 | 1053 | 891 | 904 | 606 |
| T24 | 332 | 1221 | 1220 | 1347 | 1344 | 794 | 1313 | 1323 | 1351 | 1200 |
| T25 | 311 | 1061 | 1073 | 1326 | 1264 | 838 | 1248 | 1286 | 1292 | 1189 |
| T25 | 296 | 866 | 827 | 1128 | 1066 | 712 | 964 | 984 | 773 | 569 |
| Border gap, row I | | | | | | | | | | |
| T46 | 292 | 1156 | 1215 | 1247 | 1196 | 726 | 1098 | 1081 | 863 | 324 |
| T47 | 299 | 1158 | 1181 | 1340 | 1332 | 561 | 1306 | 1326 | 1291 | 878 |
| T48 | 292 | 901 | 893 | 1129 | 1113 | 767 | 1058 | 1078 | 869 | 324 |
| Border gap, row 1 | | | | | | | | | | |
| T4 | 314 | 1424 | 1403 | 1458 | 1441 | 471 | 1417 | 1451 | 1394 | 1371 |
| T18 | 294 | 1142 | 1112 | 1213 | 1178 | 671 | 1121 | 1190 | 969 | 768 |
| T27 | 299 | 1204 | 1171 | 1298 | 1271 | 542 | 1253 | 1282 | 1236 | 1127 |
| T35 | 295 | 1225 | 1210 | 1305 | 1279 | 605 | 1252 | 1282 | 1282 | 854 |
| Border gap, row 5 | | | | | | | | | | |
| T14 | 294 | 1199 | 1196 | 1326 | 1338 | 496 | 1289 | 1340 | 1266 | 1135 |
| T22 | 294 | 1260 | 1249 | 1376 | 1358 | 706 | 1330 | 1377 | 1273 | 1122 |
| T31 | 299 | 1432 | 1405 | 1442 | 1431 | 436 | 1401 | 1436 | 1182 | 1141 |
| T45 | 281 | 1204 | 1198 | 1282 | 1259 | 499 | 1171 | 1270 | 971 | 651 |
| Interior gaps | | | | | | | | | | |
| T9 | 293 | 903 | 887 | 1271 | 1259 | 755 | 1243 | 1263 | 1296 | 1041 |
| T15 | 292 | 622 | 626 | 1008 | 979 | 816 | 952 | 972 | 934 | 483 |
| T16 | 301 | 866 | 869 | 1035 | 1009 | 891 | 988 | 1044 | 881 | 571 |
| T17 | 292 | 340 | 339 | 679 | 649 | 709 | 615 | 639 | 619 | 322 |
| T20 | 293 | 713 | 699 | 958 | 926 | 798 | 867 | 919 | 834 | 419 |
| T32 | 293 | 337 | 331 | 876 | 853 | 836 | 822 | 852 | 827 | 320 |
| T33 | 296 | 767 | 717 | 1018 | 997 | 833 | 983 | 1009 | 976 | 558 |
| T34 | 294 | 656 | 665 | 1015 | 980 | 856 | 948 | 998 | 891 | 392 |
| T40 | 292 | 531 | 599 | 936 | 916 | 780 | 894 | 939 | 963 | 351 |

TABLE V. - PANEL TEMPERATURES (K) AFTER 30 s OF AERODYNAMIC HEATING FOR MODE II AND 40 s OF AERODYNAMIC HEATING FOR MODE III - Concluded
(c) Substructure

| Thermo- couple no. | Test no. | | | | | | | | | |
|---------------------------------------|----------|-----|-----|-----|-----|-----|-----|-----|-----|-----|
| | 3 | 5 | 6 | 8 | 10 | 11 | 12 | 15 | 22 | 23 |
| Beryllium subpanel skin (z = 3.50 cm) | | | | | | | | | | |
| T81 | 293 | 295 | 294 | 388 | 372 | 393 | 358 | 360 | 409 | 295 |
| T82 | 293 | 295 | 294 | 391 | 374 | 394 | 360 | 362 | 411 | 295 |
| T85 | 294 | 298 | 296 | 403 | 383 | 406 | 371 | 372 | 419 | 298 |
| Titanium frame (z = 6.78 cm) | | | | | | | | | | |
| T59 | 293 | 334 | 324 | 399 | 373 | 339 | 56 | 388 | 351 | 292 |
| T61 | 292 | 391 | 403 | 443 | 416 | 328 | 402 | 442 | 371 | 311 |
| T63 | 293 | 412 | 405 | 365 | 347 | 344 | 336 | 353 | 353 | 304 |
| T65 | 292 | 536 | 519 | 534 | 549 | 337 | 507 | 582 | 353 | 296 |
| T67 | 292 | 304 | 302 | 350 | 337 | 327 | 327 | 332 | 347 | 305 |
| T69 | 292 | 331 | 331 | 393 | 387 | 332 | 367 | 387 | 357 | 299 |
| T71 | 292 | 322 | 316 | 363 | 357 | 328 | 343 | 359 | 339 | 305 |
| Titanium frame (z = 12.6 cm) | | | | | | | | | | |
| T60 | 292 | 292 | 293 | 311 | 306 | 305 | 296 | 297 | 313 | 291 |
| T62 | 292 | 292 | 293 | 310 | 306 | 304 | 294 | 297 | 314 | 291 |
| T64 | 292 | 292 | 293 | 313 | 307 | 306 | 297 | 298 | 316 | 291 |
| T66 | 292 | 293 | 292 | 310 | 306 | 304 | 297 | 299 | 314 | 291 |
| T68 | 292 | 293 | 293 | 309 | 304 | 305 | 295 | 297 | 312 | 291 |
| T70 | 292 | 291 | 290 | 309 | 304 | 304 | 296 | 297 | 313 | 292 |
| T72 | 291 | 292 | 291 | 311 | 307 | 302 | 296 | 299 | 309 | 292 |
| T74 | 292 | 292 | 291 | 309 | 303 | 302 | 296 | 297 | 309 | 291 |
| Aluminum base plate (z = 12.7 cm) | | | | | | | | | | |
| T77 | 292 | 293 | 295 | 318 | 314 | 309 | 302 | 308 | 322 | 290 |
| T78 | 292 | 293 | 293 | 318 | 311 | 308 | 303 | 306 | 317 | 292 |

REPRODUCIBILITY OF THE ORIGINAL PAGE IS POOR.

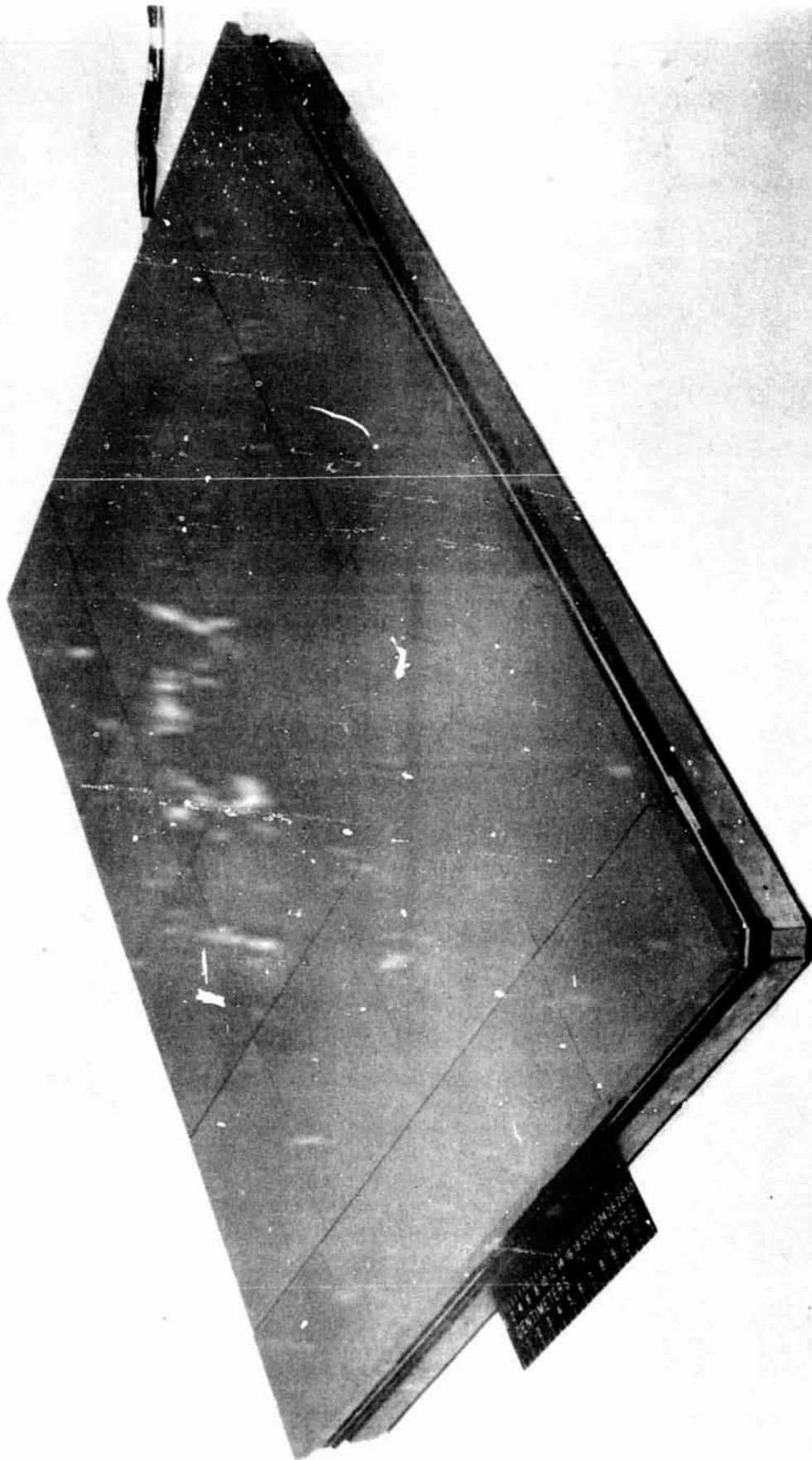


Figure 1. - Photograph of test panel with RSI tiles.

REPRODUCIBILITY OF THE ORIGINAL PAGE IS POOR.

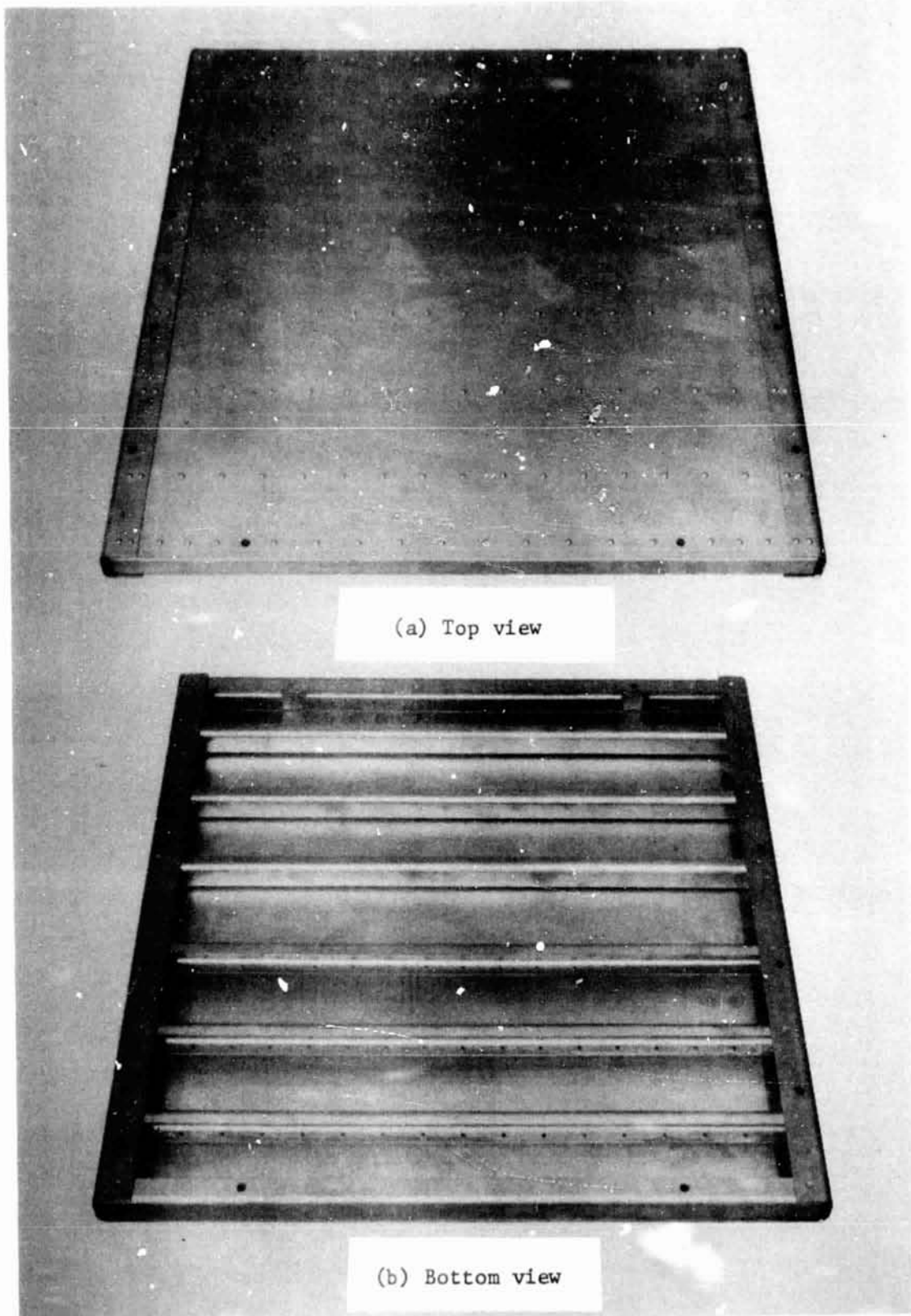
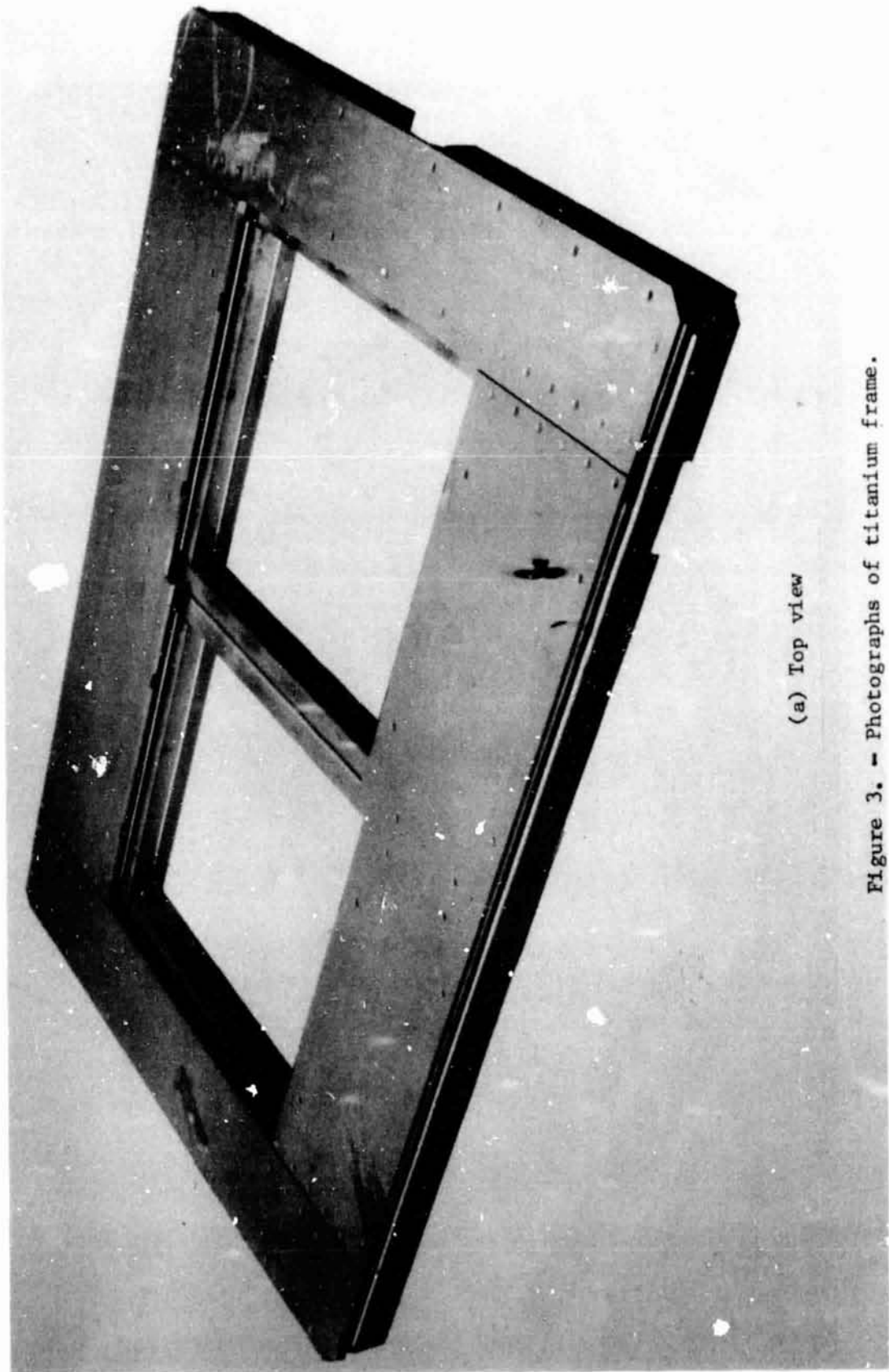


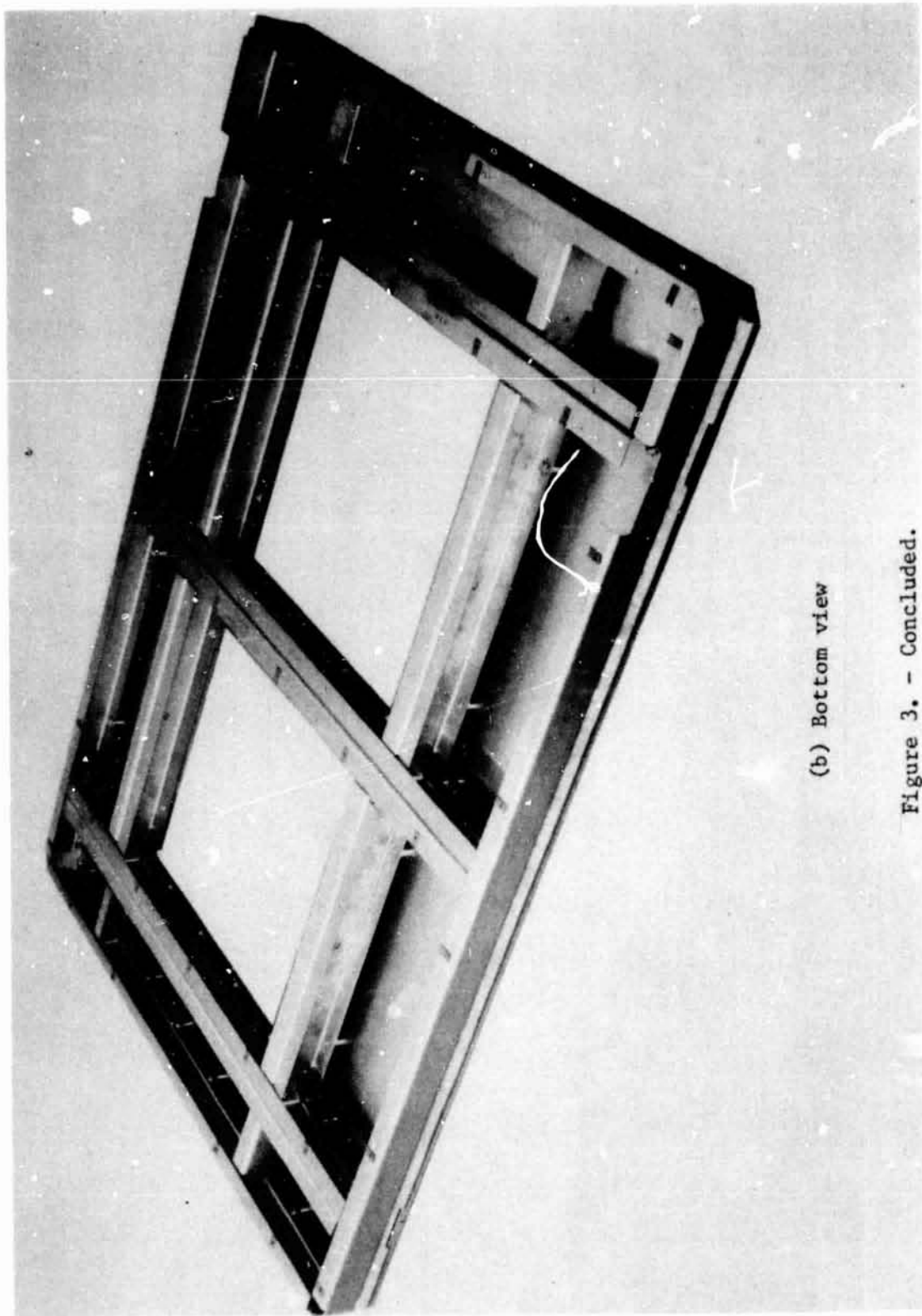
Figure 2. - Photographs of stringer-stiffened beryllium subpanel.



(a) Top view

Figure 3. - Photographs of titanium frame.

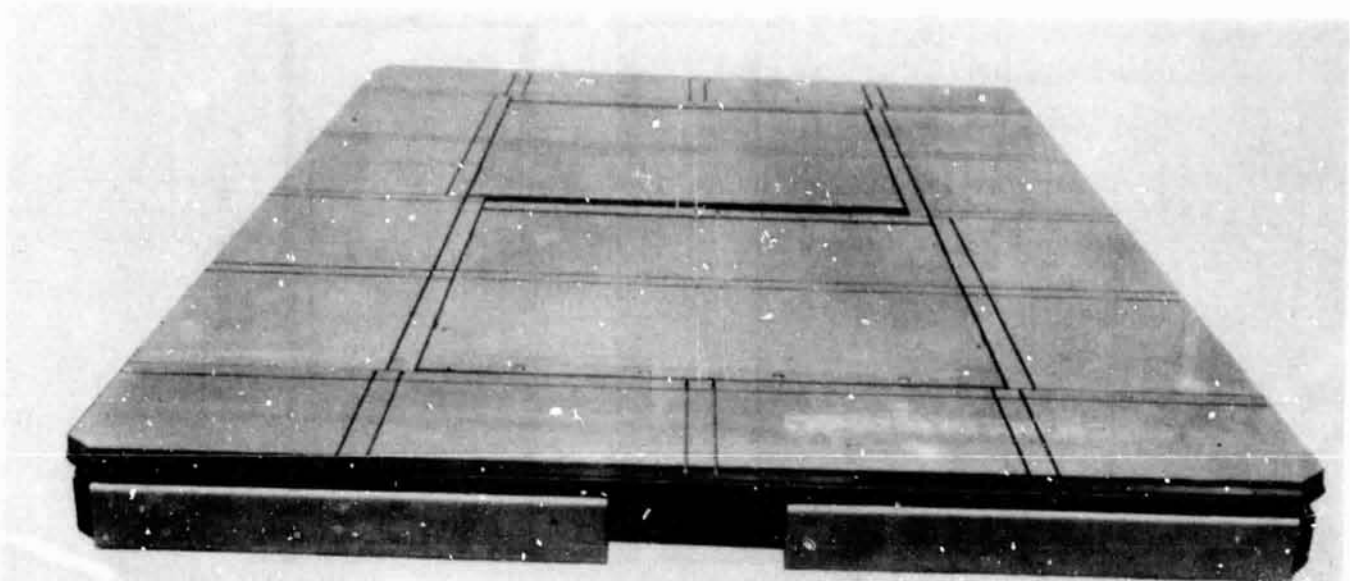
REPRODUCIBILITY OF THE ORIGINAL PAGE IS POOR.



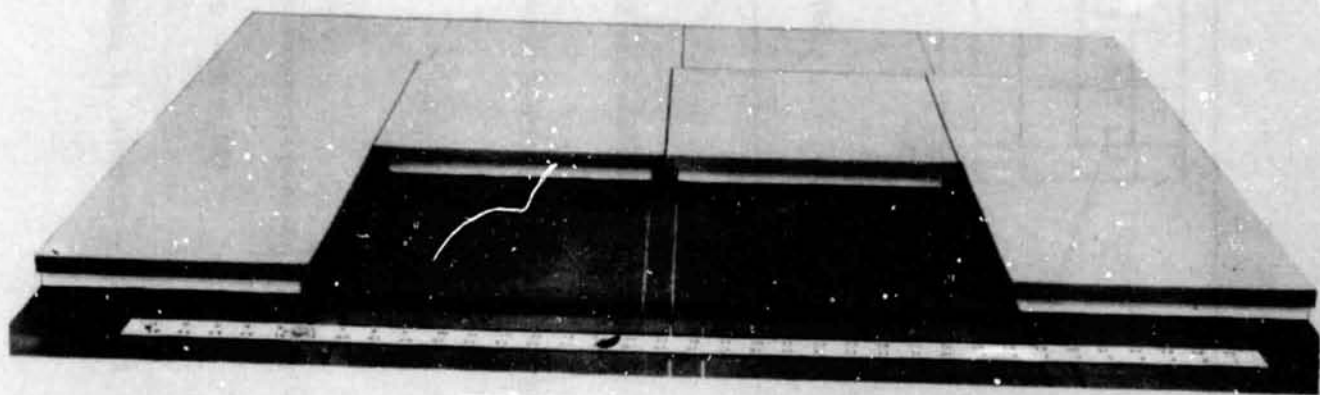
(b) Bottom view

Figure 3. - Concluded.

REPRODUCIBILITY OF THE ORIGINAL PAGE IS POOR.



(a) Substructure with RTV bond.



(b) Tile position

Figure 4. - Photographs illustrating tile assembly.

REPRODUCIBILITY OF THE ORIGINAL PAGE IS POOR.

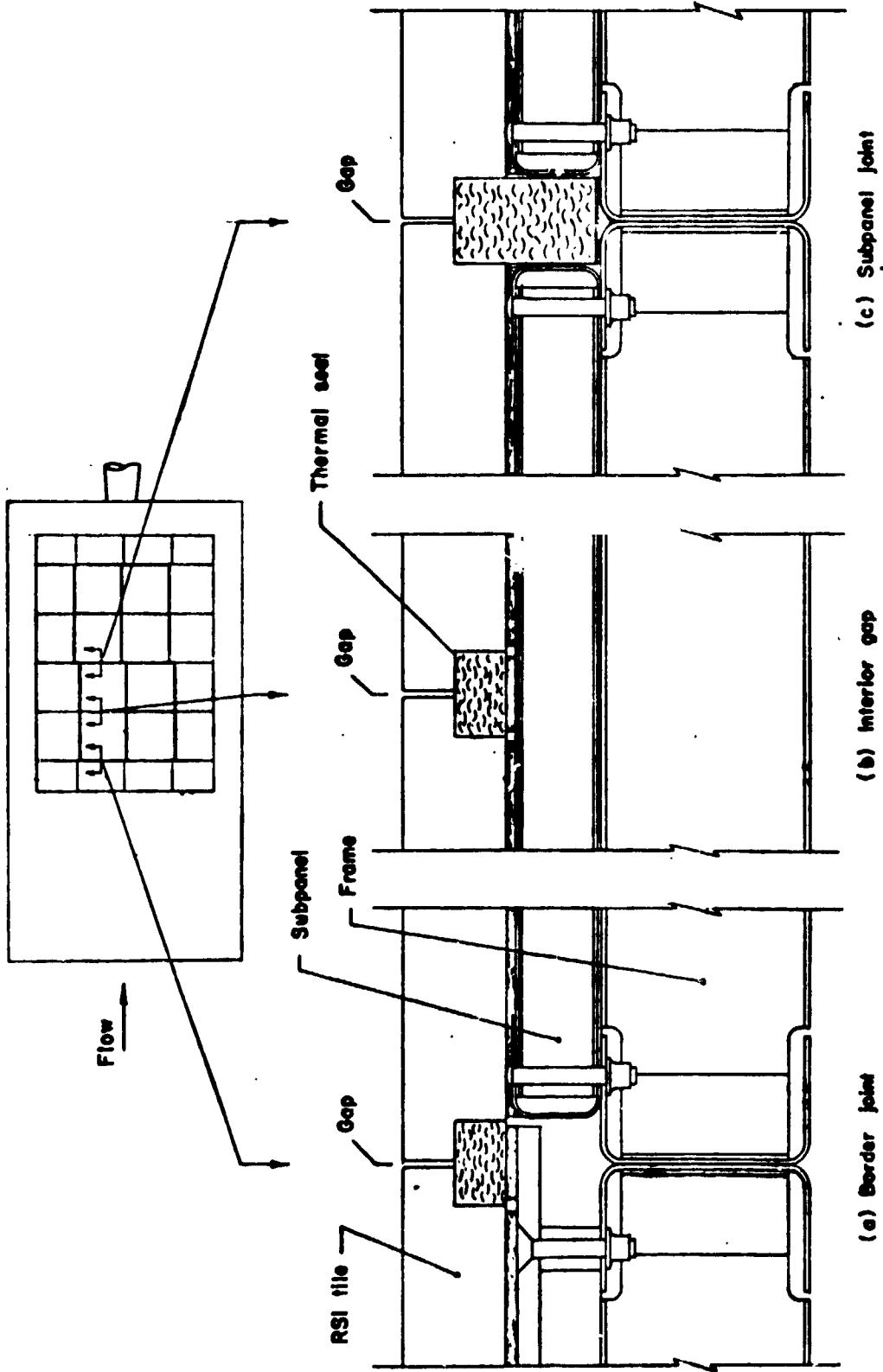


Figure 5. — Schematic of panel tiles and joints.

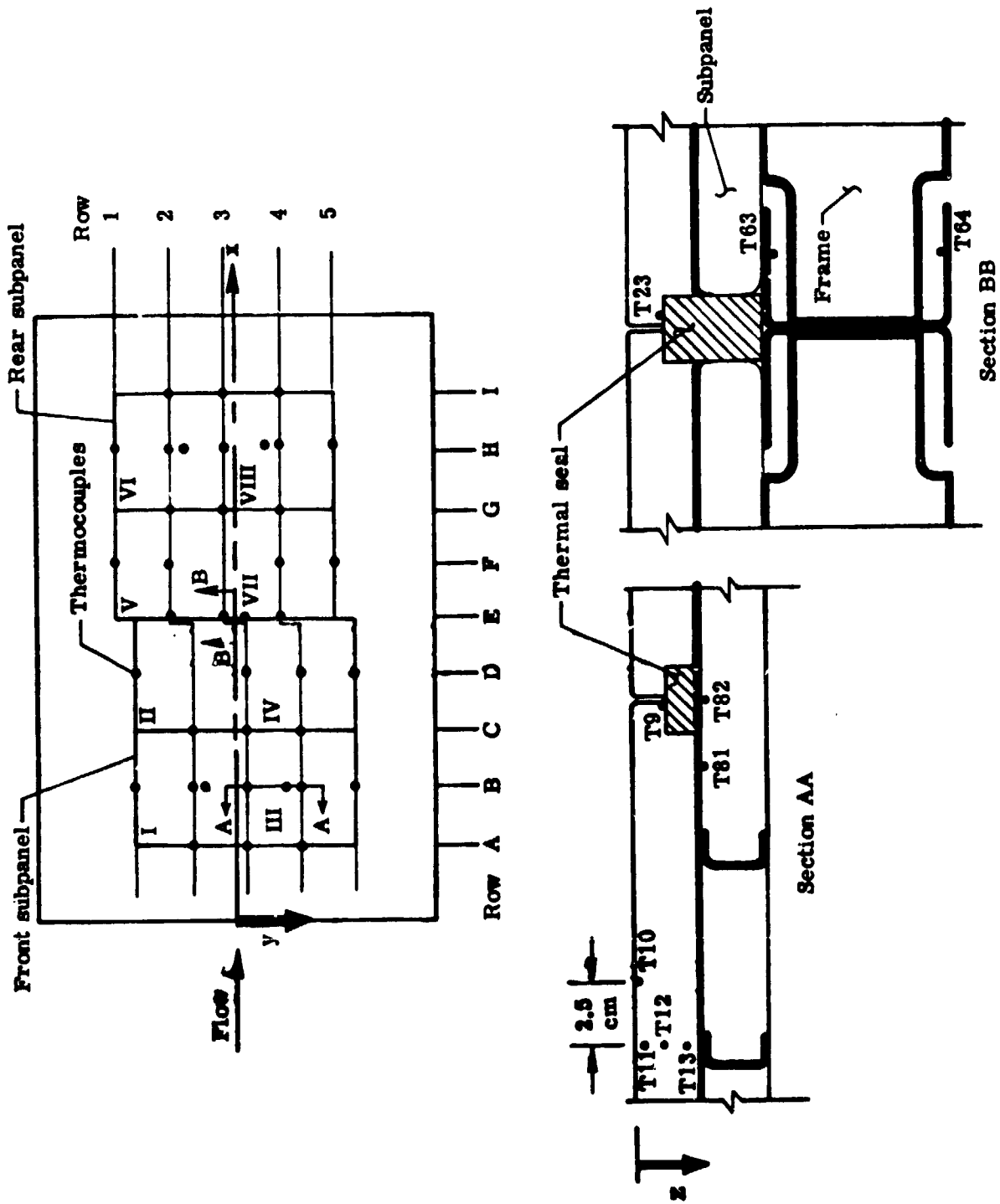


Figure 6.- Sketch of panel structure with thermocouple locations indicated.

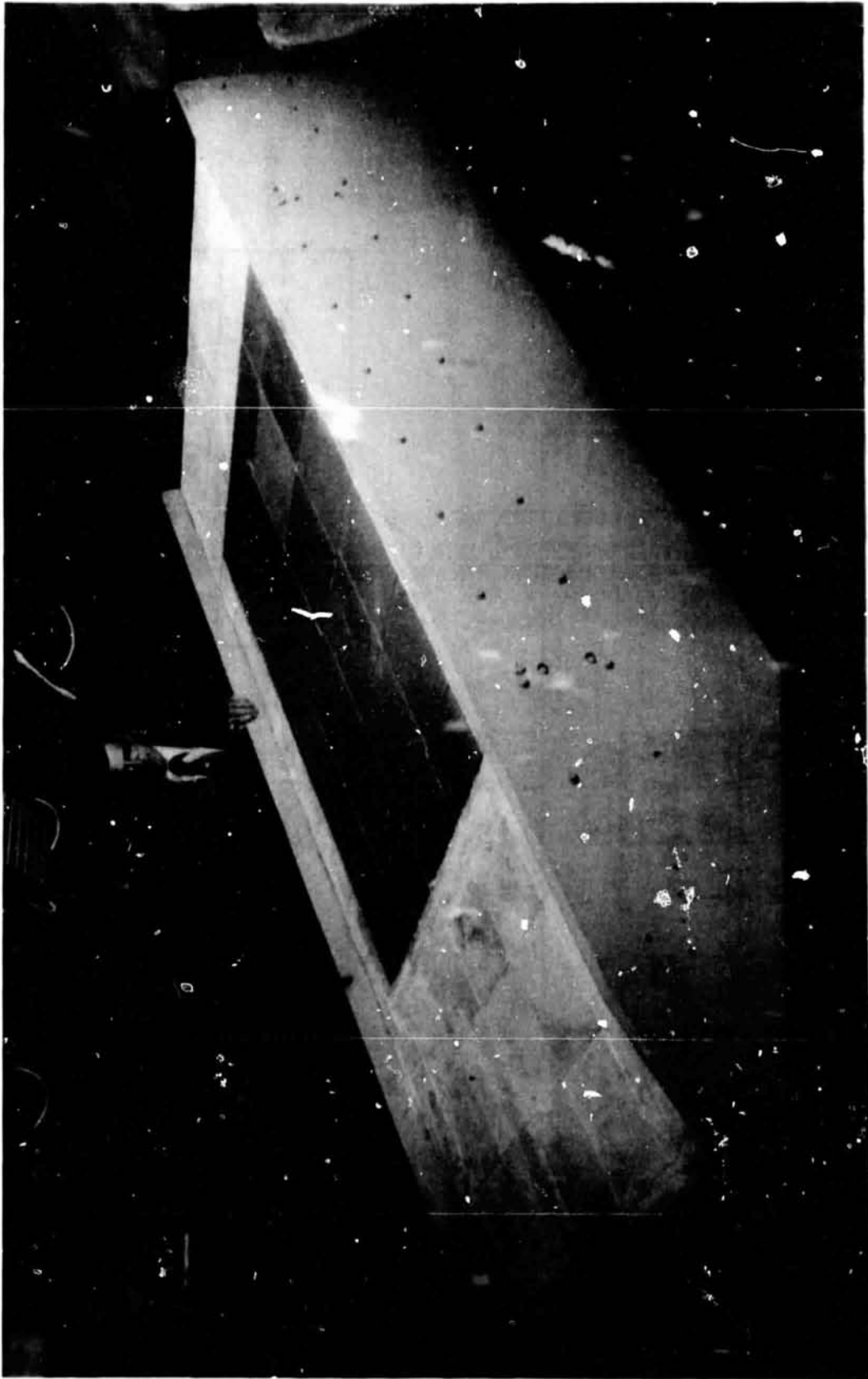


Figure 7. - Photograph of test panel installed in the 8-foot HTST panel holder.

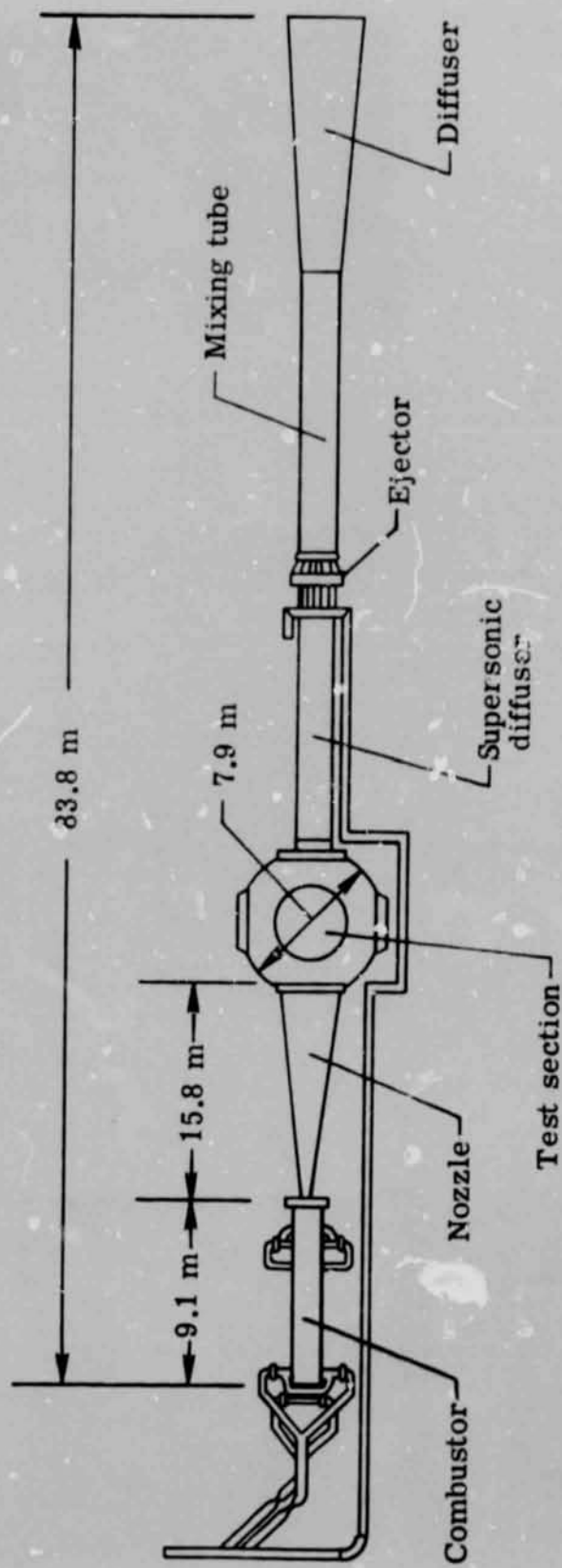


Figure 8.- Schematic drawing of the Langley 8-foot high-temperature structure tunnel.

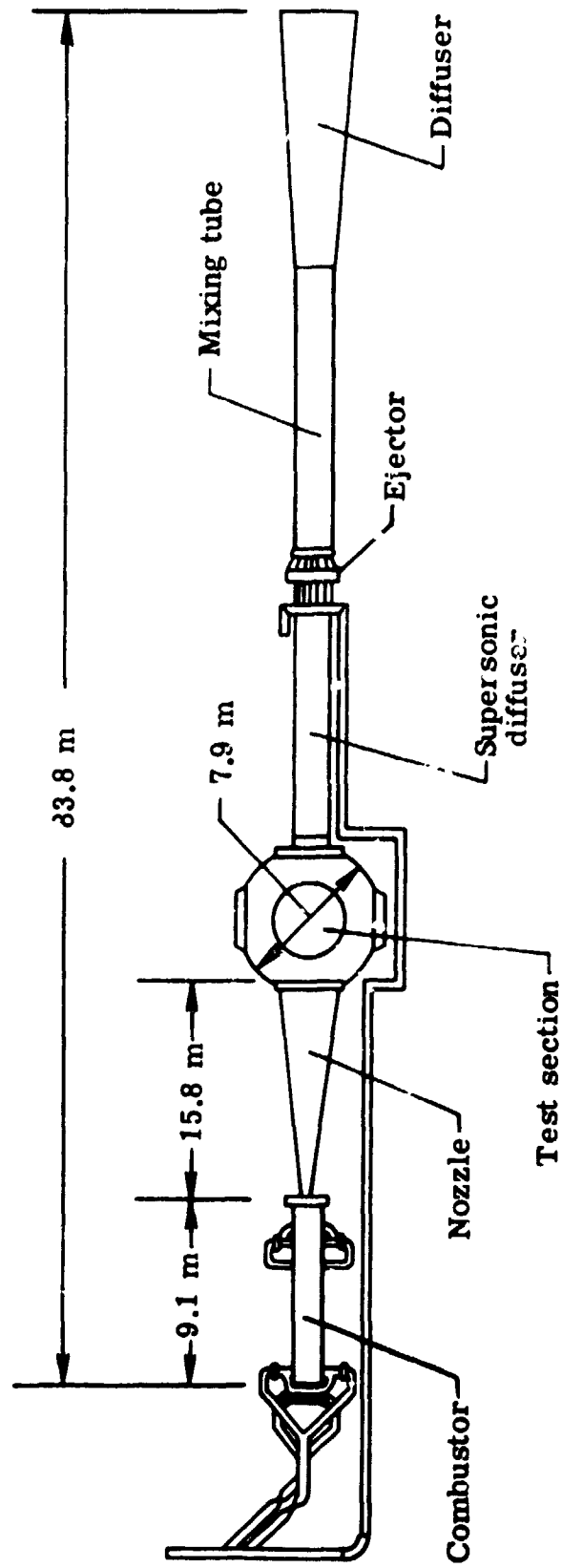


Figure 8.- Schematic drawing of the Langley 8-foot high-temperature structure tunnel.

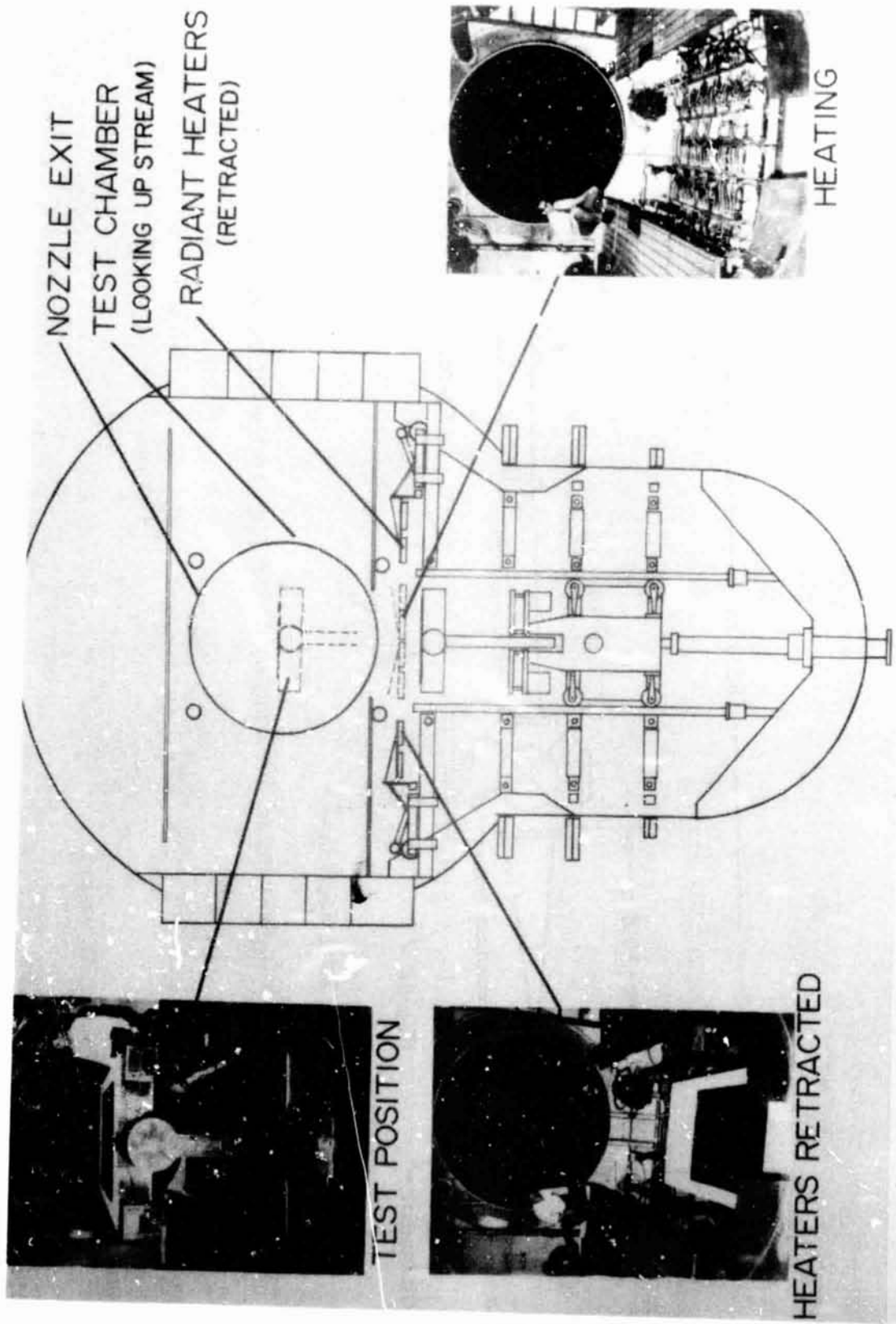
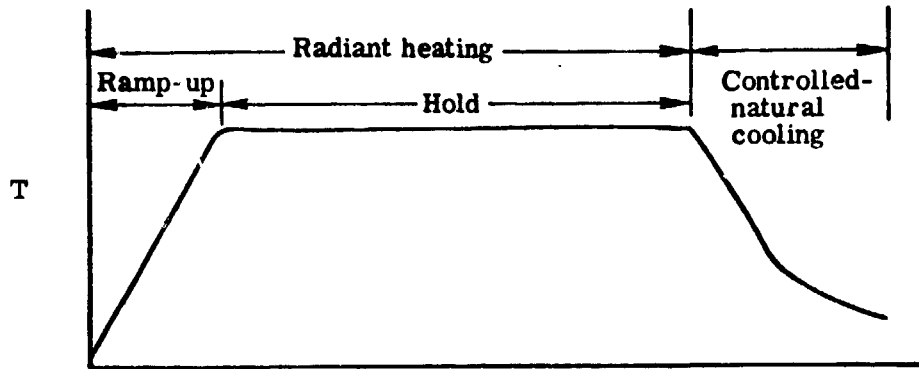
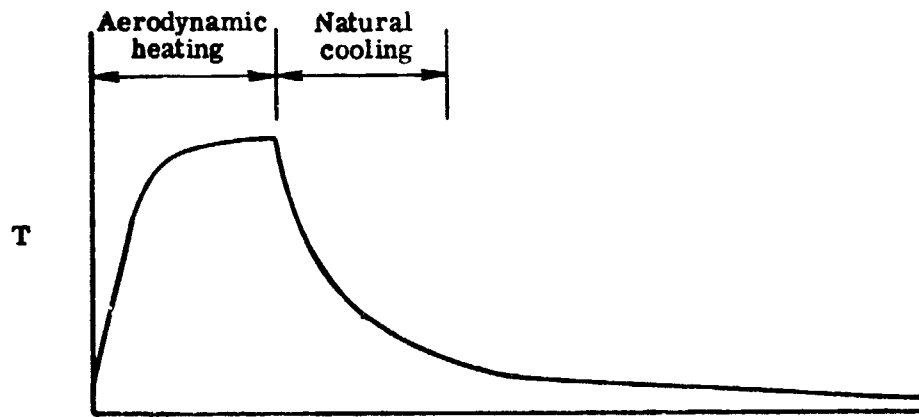


Figure 9. - Illustration of radiant heating apparatus in the 8-foot TST.

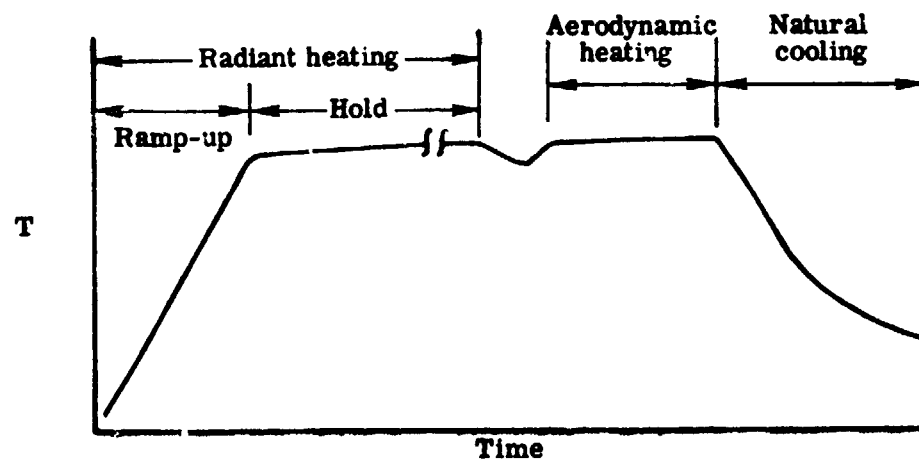
REPRODUCIBILITY OF THE ORIGINAL PAGE IS POOR.



(a) Radiant heating (Mode I).



(b) Aerodynamic heating (Mode II).



(c) Radiant heating and aerodynamic heating (Mode III).

Figure 10.- Typical surface temperature history test modes.

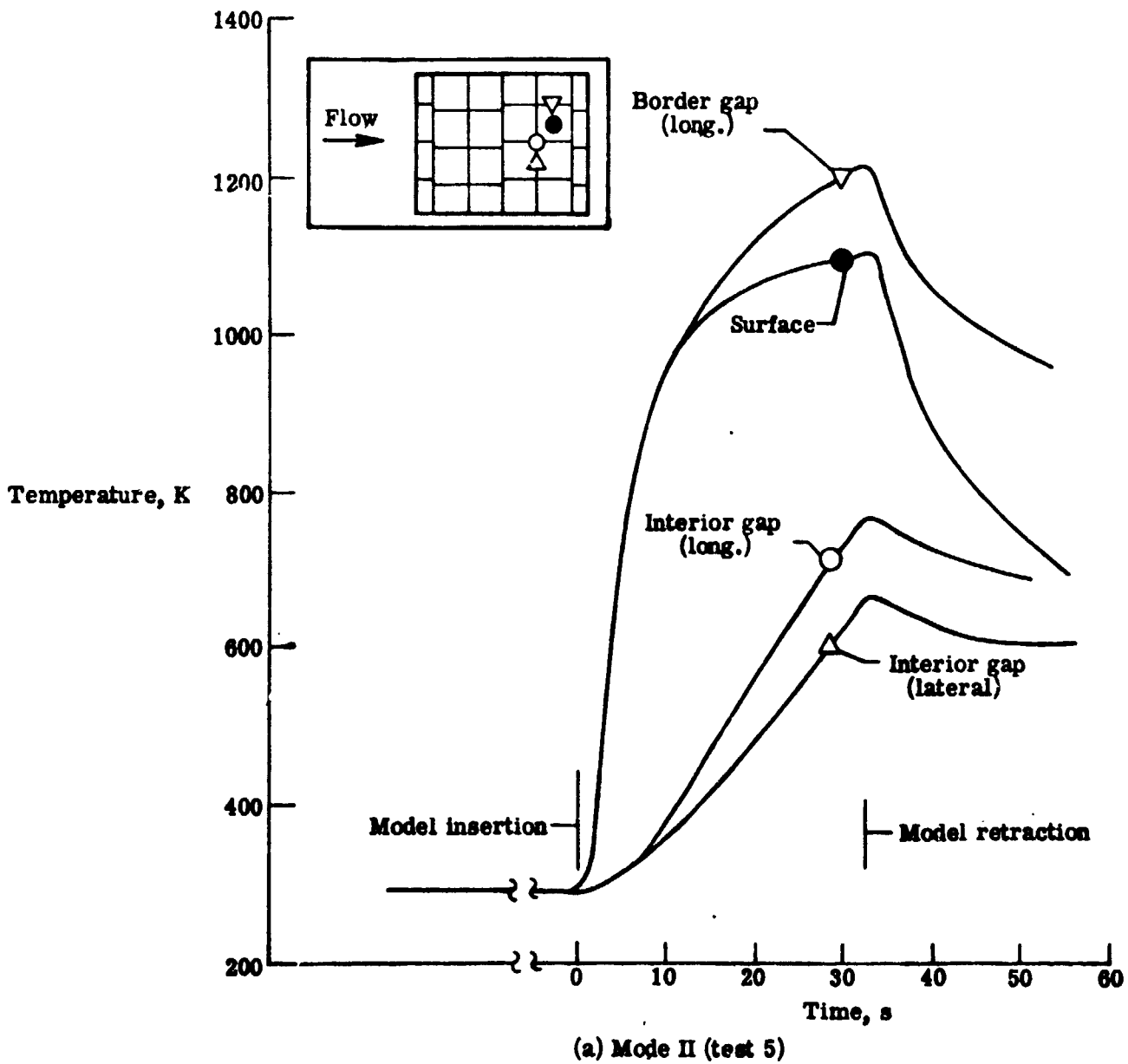
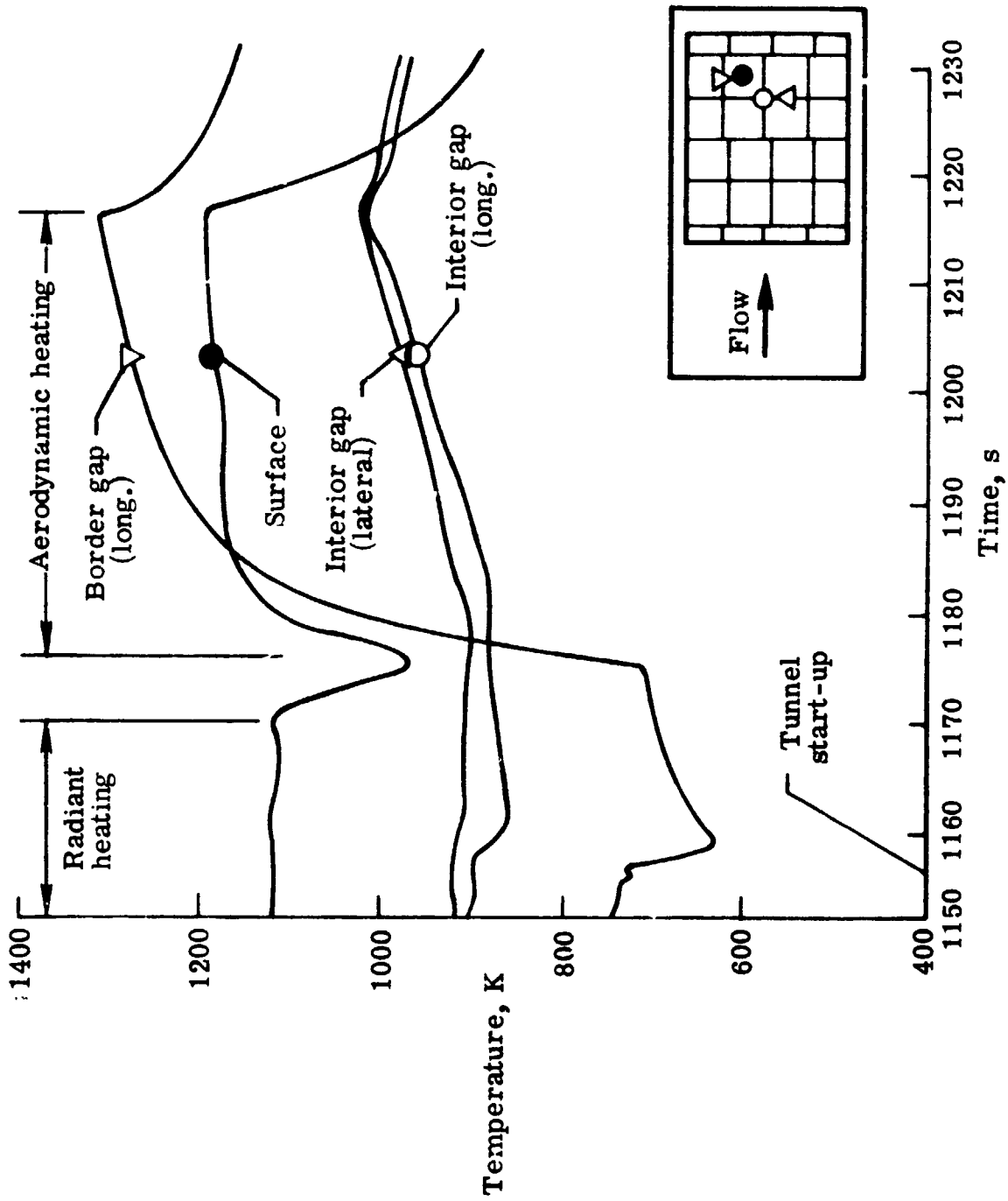
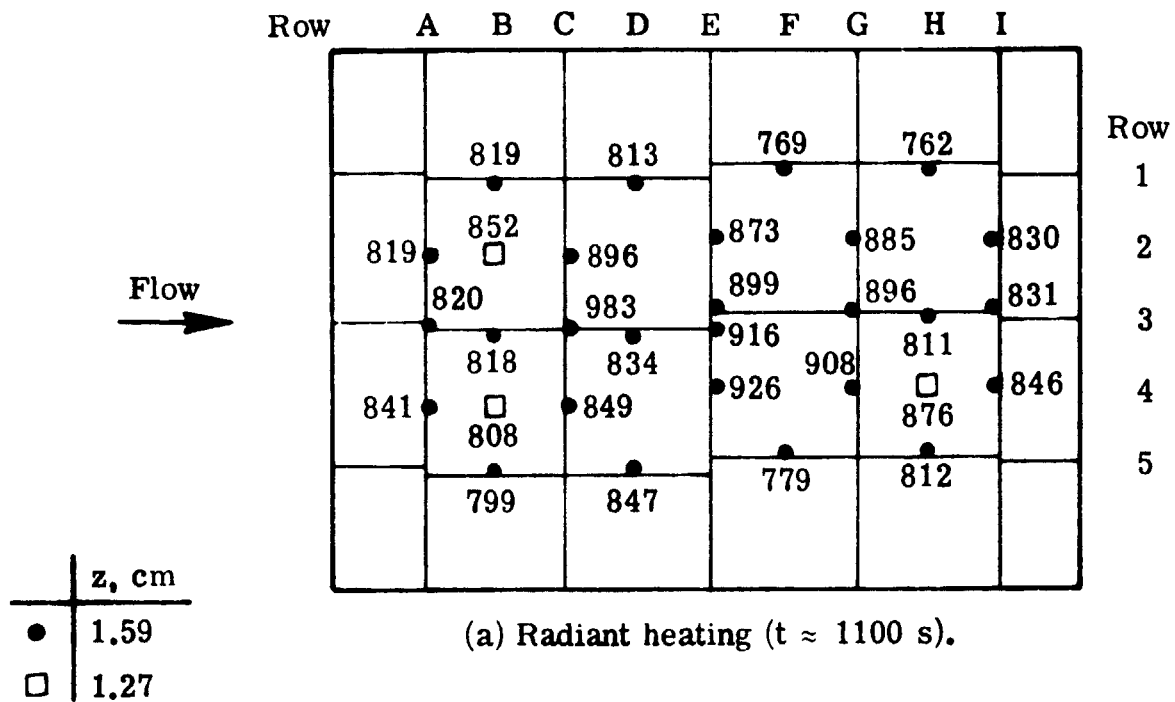


Figure 11.- Typical thermal response of panel to aerodynamic heating.

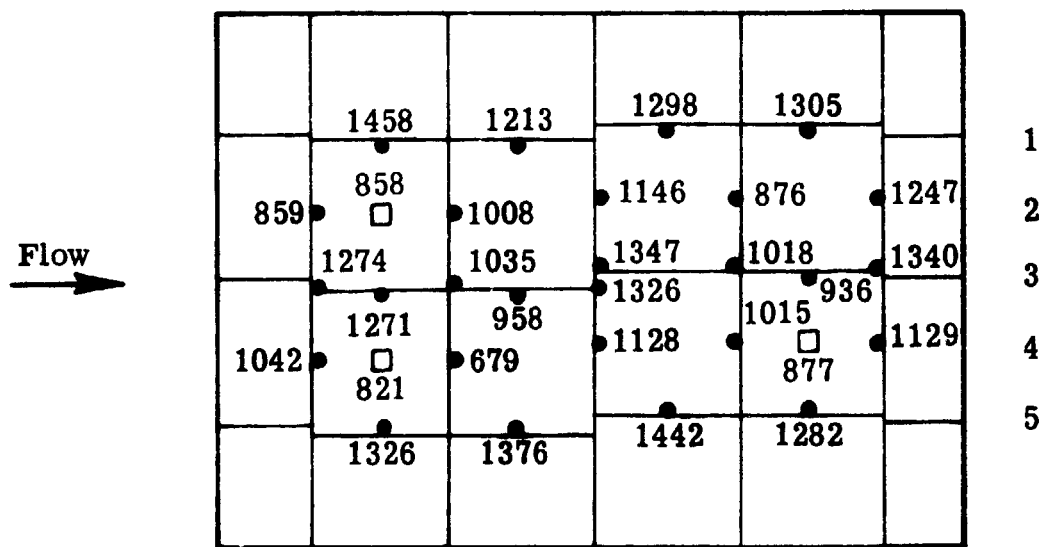


(b) Mode III (test 8)

Figure 11.- Concluded.



(a) Radiant heating ($t \approx 1100$ s).



(b) Aerodynamic heating ($t = 1215$ s)

Figure 12.- Typical temperatures (K) for mode III test (test 8).

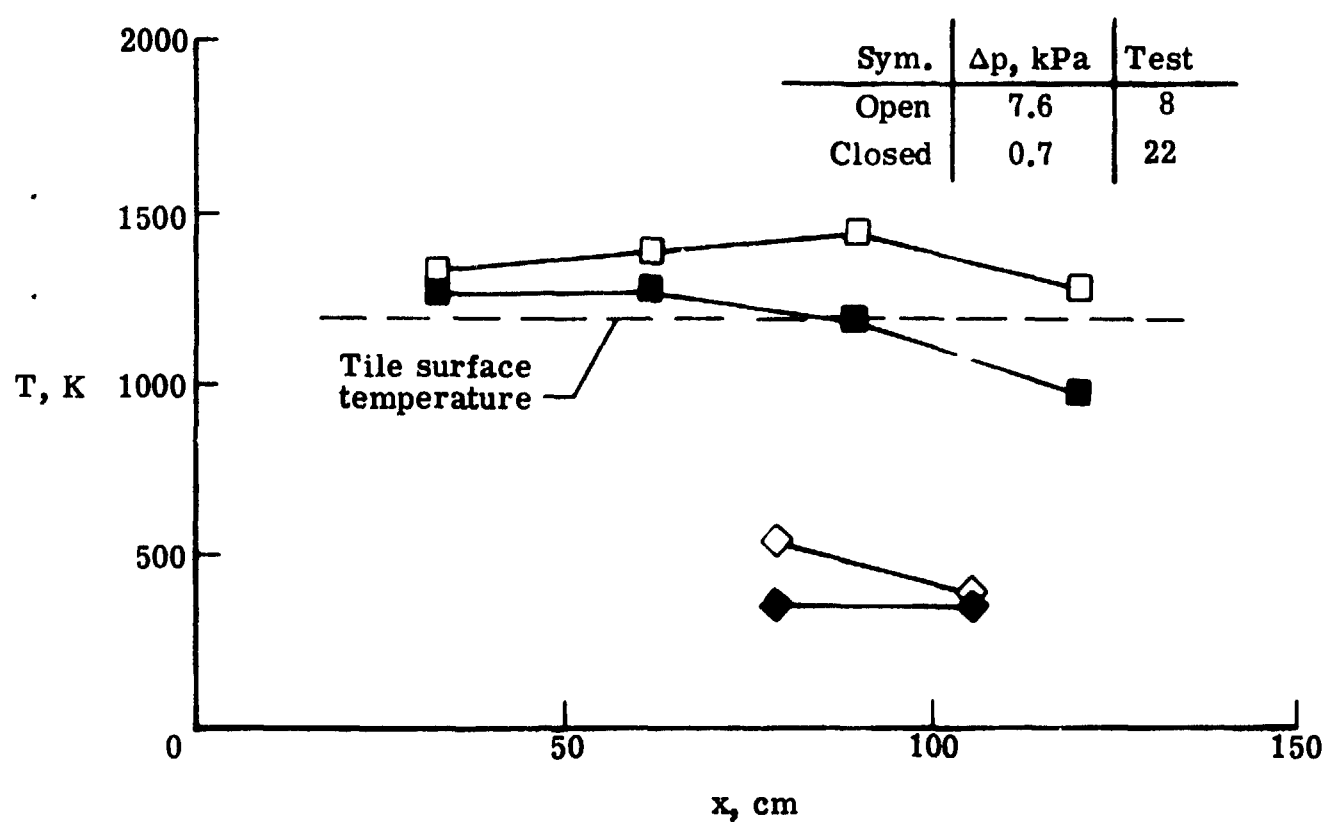
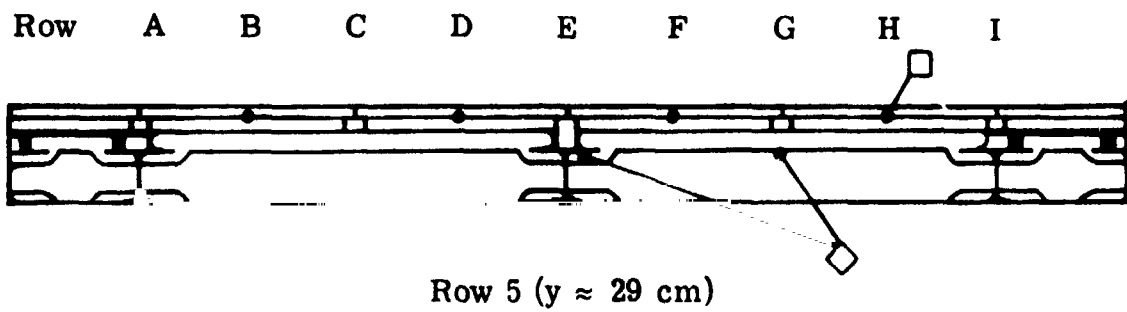


Figure 13.- Effects of differential pressure on gap and substructure temperature along row 5 after 40 s of aerodynamic heating.

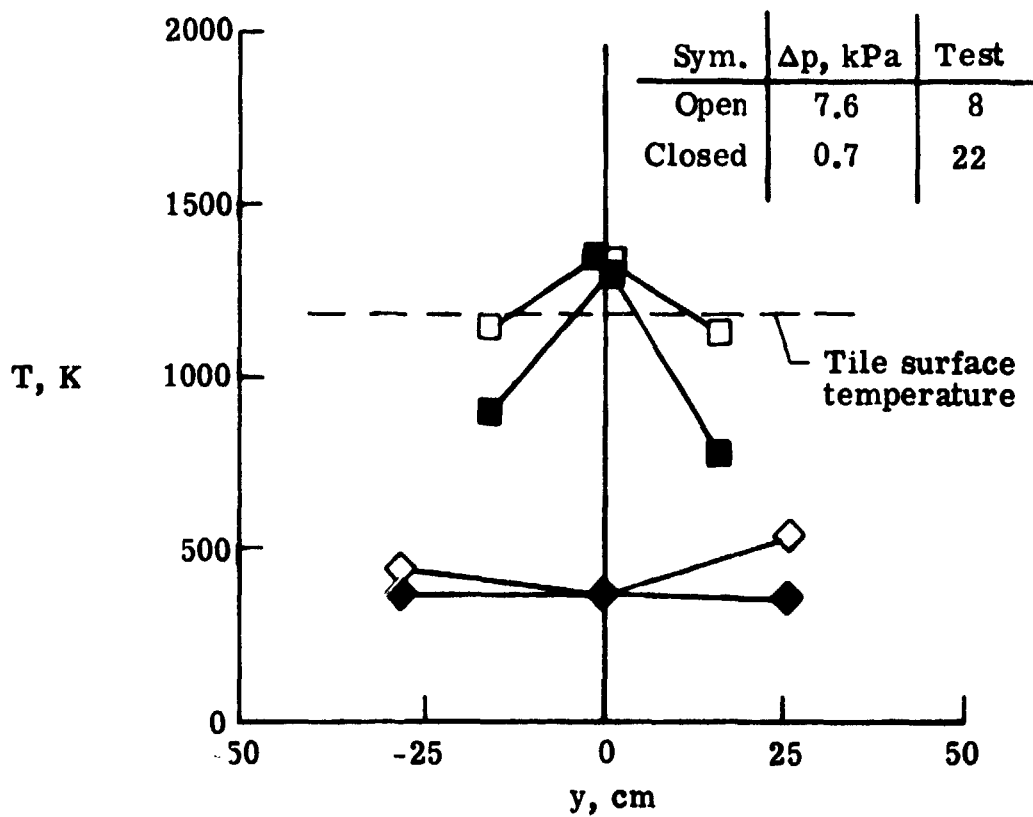
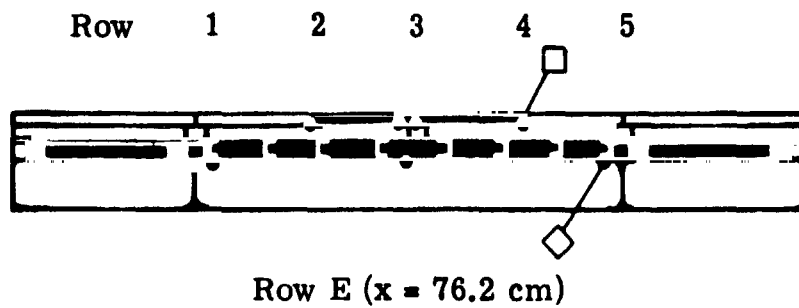


Figure 14.- Effects of differential pressure on subpanel gap and substructure temperature along row E after 40 s of aerodynamic heating.

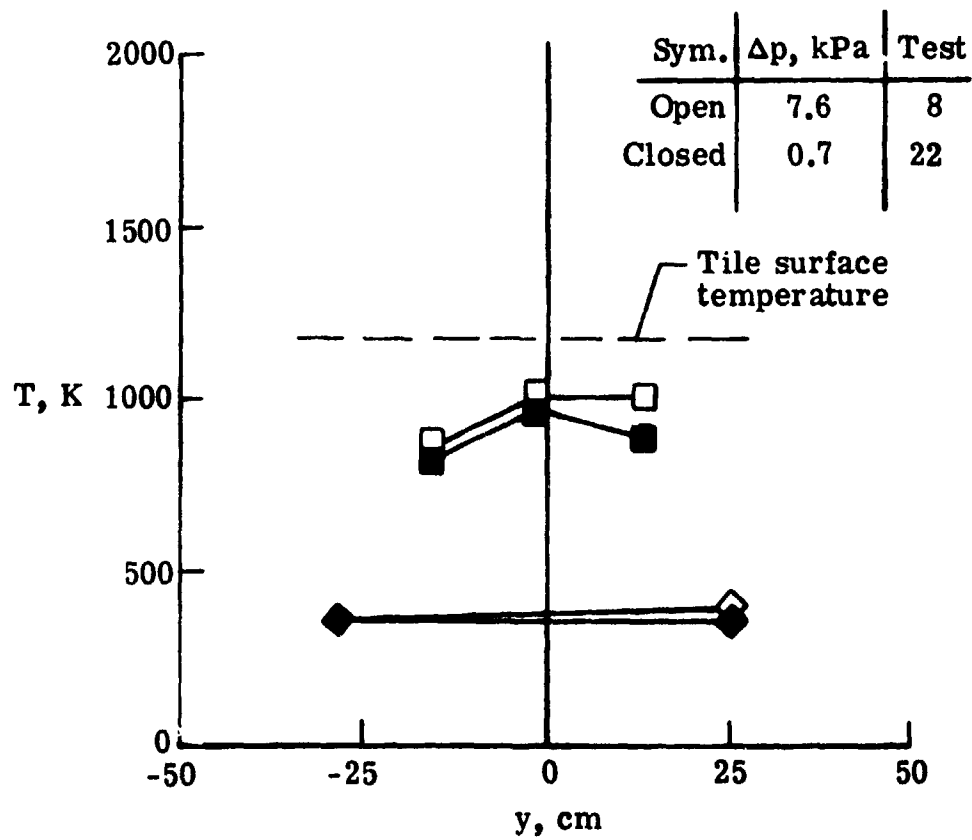
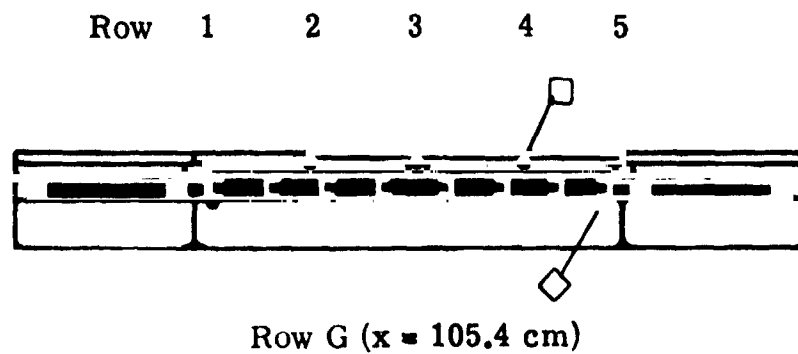


Figure 15.- Effects of differential pressure on interior gap and substructure temperature along row G after 40 s of aerodynamic heating.

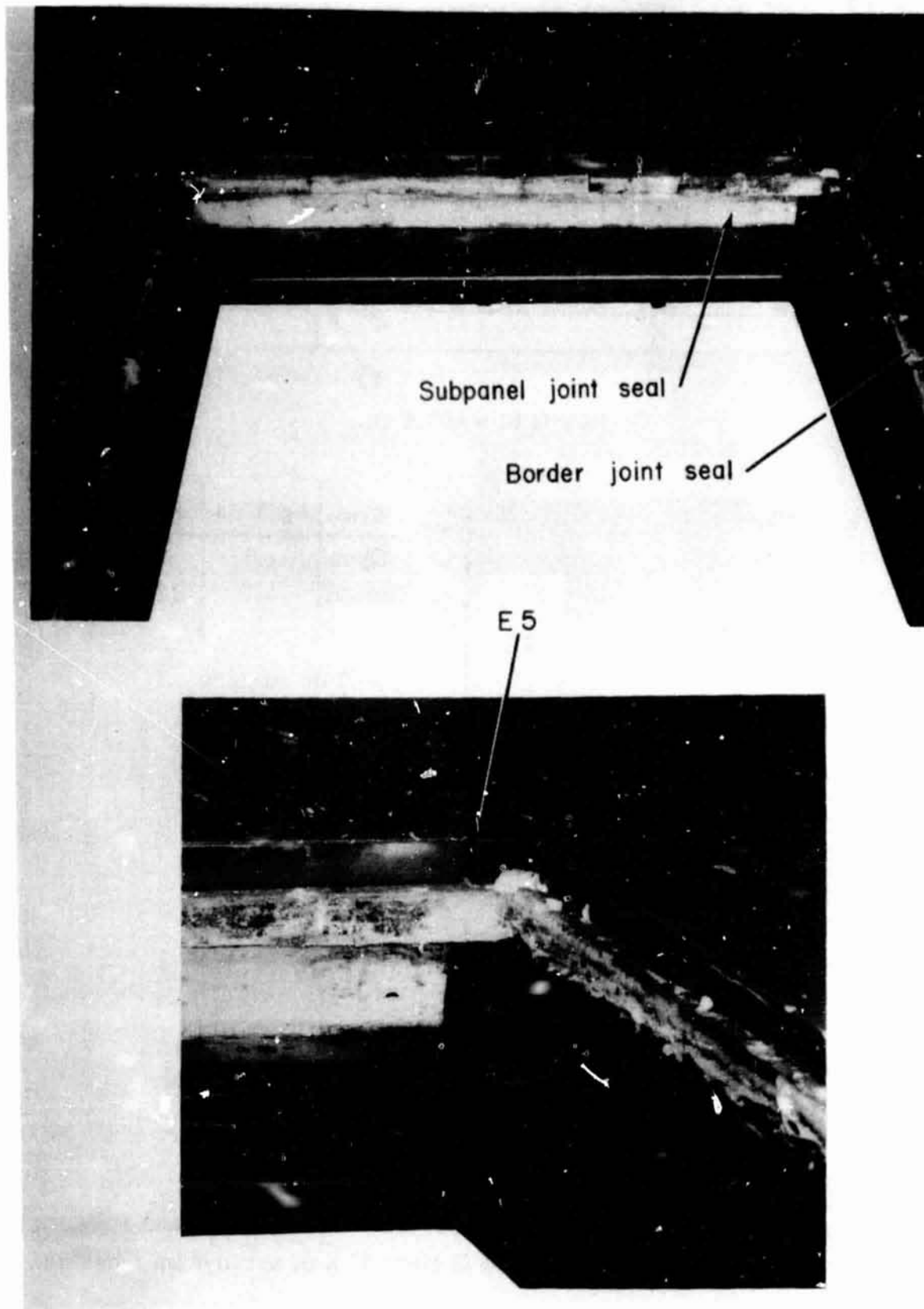


Figure 16. - Photographs of thermal seals of subpanel joint E5 at conclusion of tests.

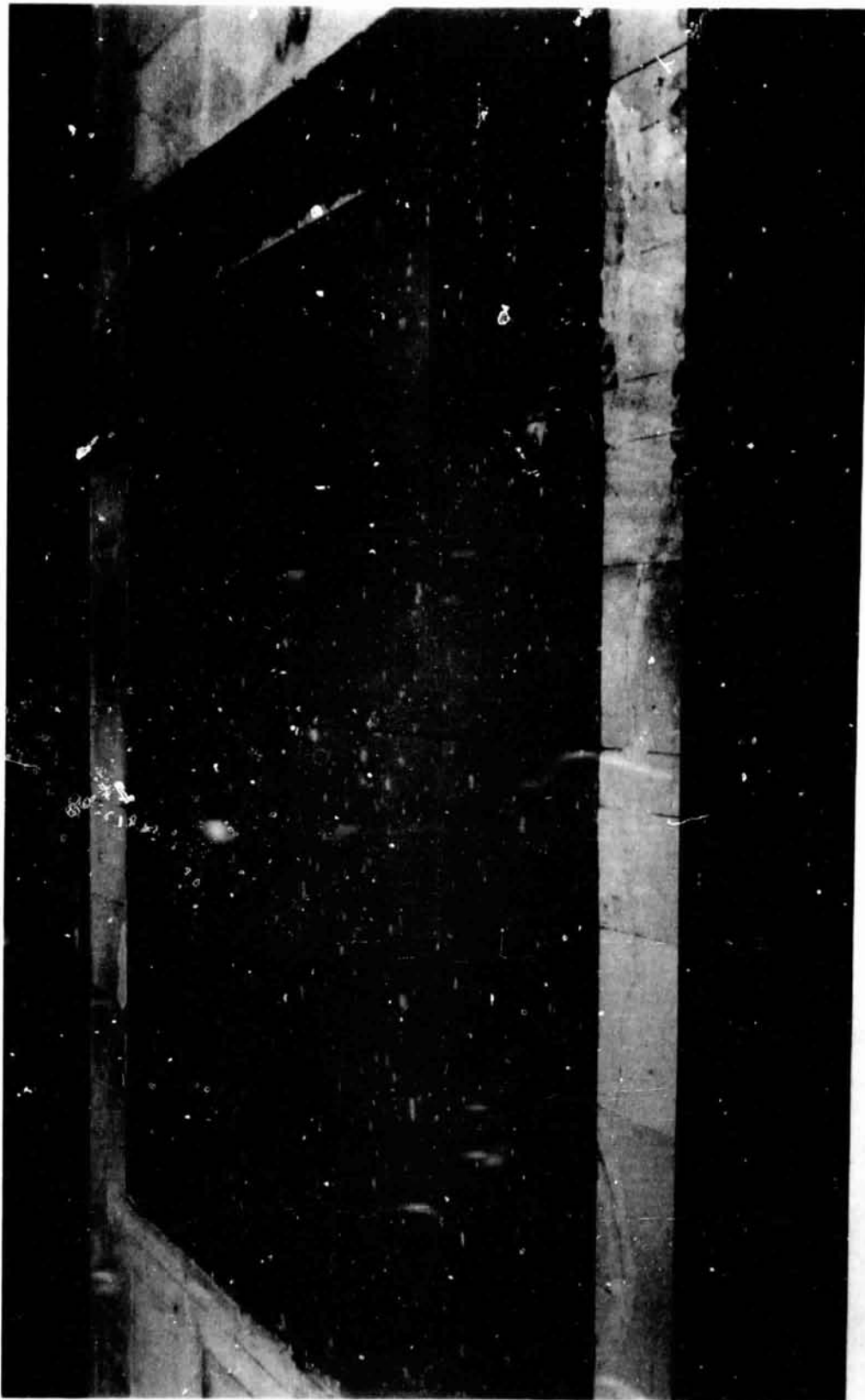
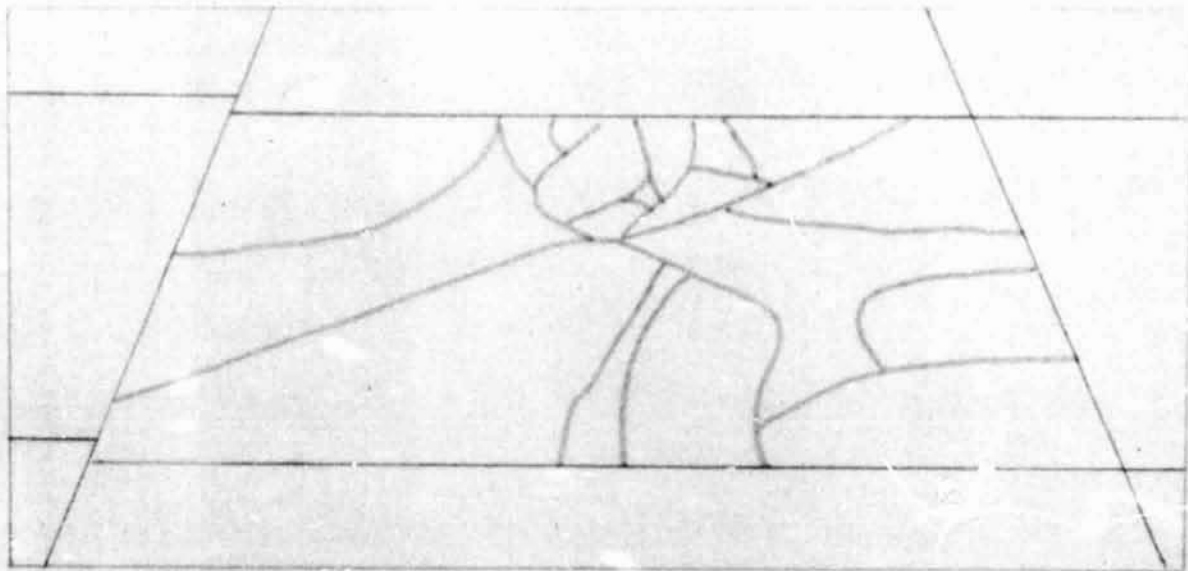


Figure 17. - Overall appearance of tile surface at conclusion of tests.



(a) Pre-test 4



(b) Post-test 4

Figure 18. - Crack patterns of tile coating (tile III).

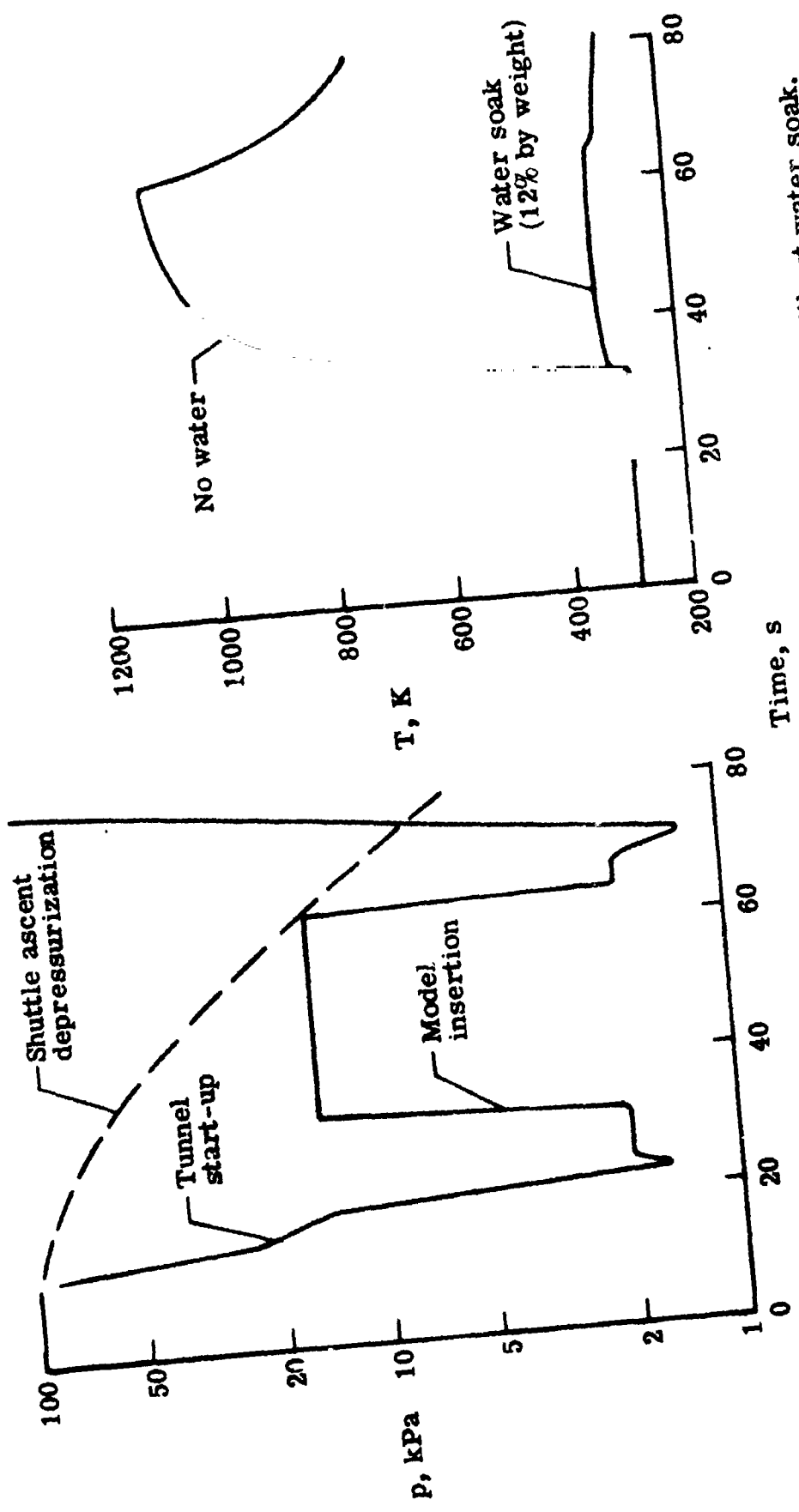


Figure 19.- Pressure-temperature history of LI-1542 tile with and without water soak.

REPRODUCIBILITY OF THE ORIGINAL PAGE IS POOR.

Flow
→



(a) Post-test 8

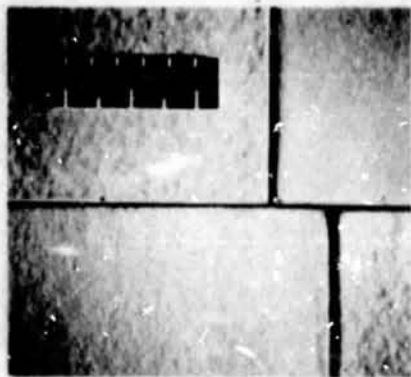


(b) Post-test 12

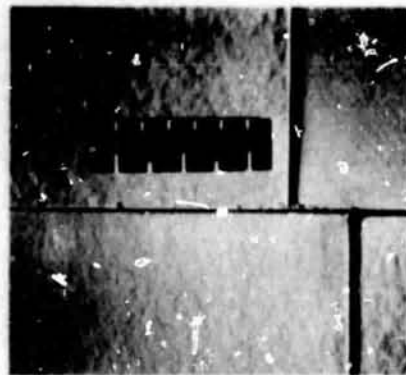


(c) Post-test 23

Figure 20. - History of crater damage and repair.



(a) Post test 2



(b) Post test 13

Figure 21. - Tile edge erosion of 0.6 mm forward-facing step at E3.

REPRODUCIBILITY OF THE ORIGINAL PAGE IS POOR.

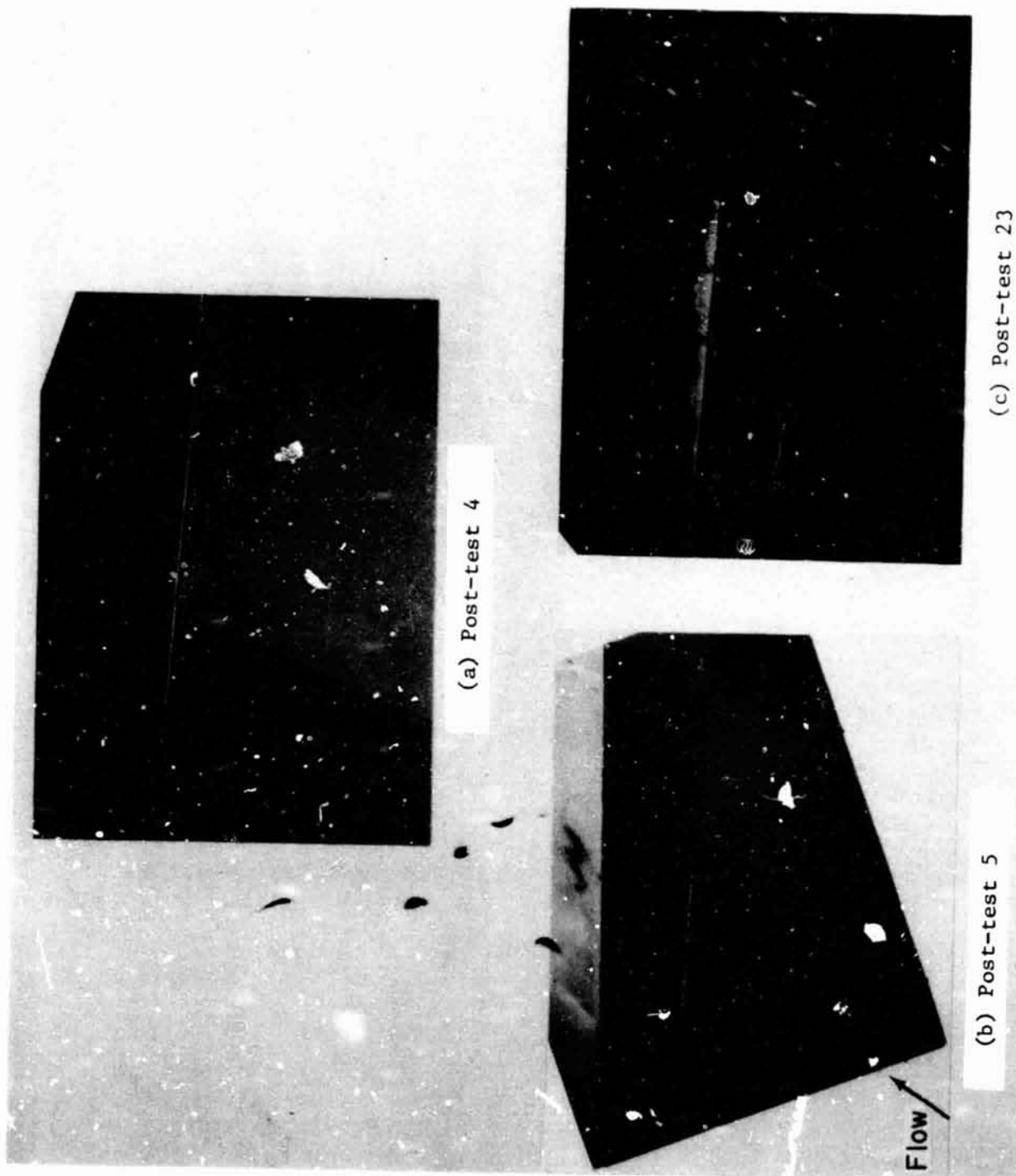


Figure 22. - Tile edge erosion of 0.4 mm forward-facing step along row I.

REPRODUCIBILITY OF THE ORIGINAL PAGE IS POOR.

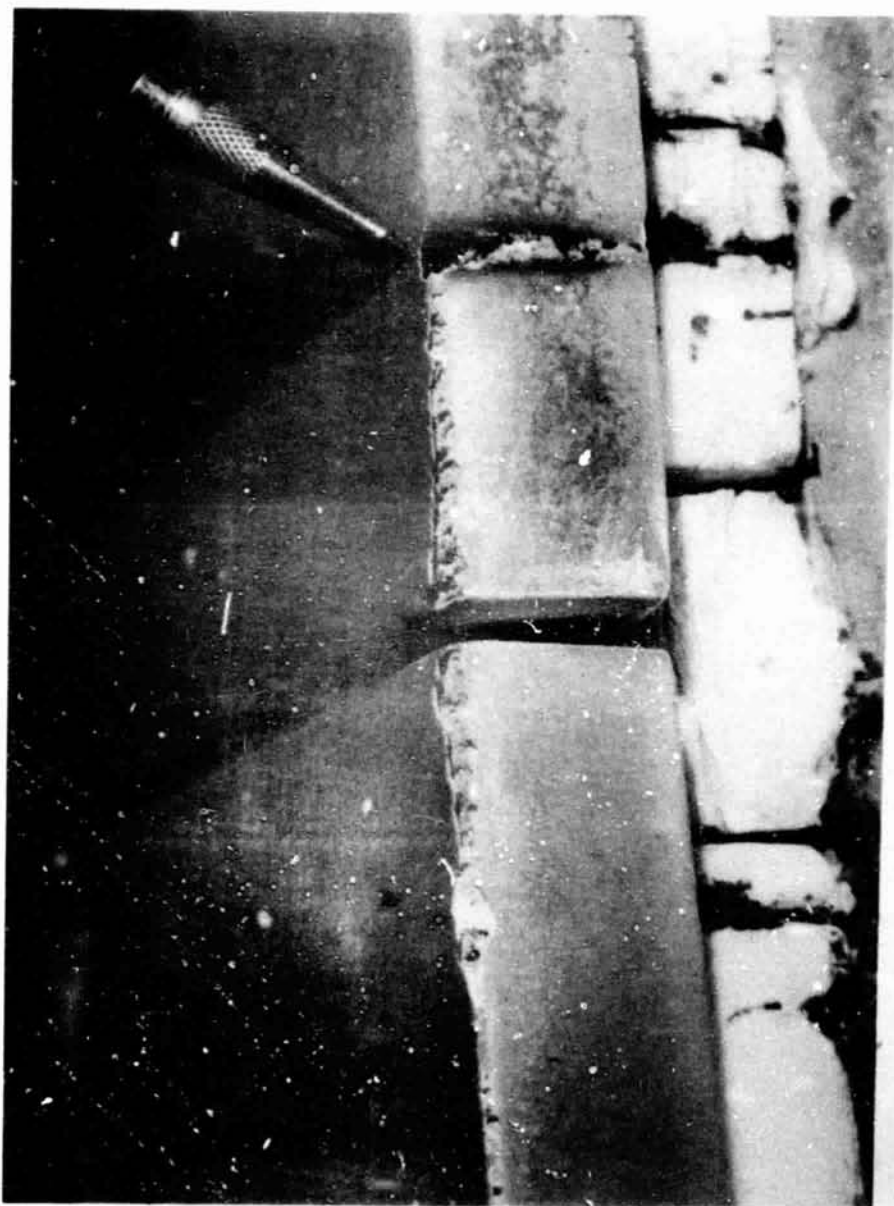


Figure 23. - Flow impingement damage of header at E3.